University of Venda

ANALYSIS OF THE PEAK POWER OF A PHOTOVOLTAIC ARRAY SYSTEM UNDER OUTDOOR CONDITIONS AT VUWANI REGION OF LIMPOPO PROVINCE

A Dissertation Submitted to the Department of Physics

For the fulfilment of a M.Sc. Degree

By

NEKHUBVI VHUTSHILO 1ST MOUNTAINEER

(11520748)

In the School of Mathematical and Natural Sciences,

University of Venda

THOHOYANDOU, LIMPOPO PROVINCE

Supervisor : Prof. V. Sankaran

MARCH 2012

DECLARATION

I, NEKHUBVI VHUTSHILO 1ST MOUNTAINEER, hereby declare that the dissertation for the M.Sc. degree at the University of Venda, hereby submitted by me, has not previously been submitted for a degree at this or any other university and that it is my own work in design and execution, and all the reference materials contained therein has been duly acknowledged.

Signature: .....Date: 31-JAN-2013

Acknowledgement

Firstly I want to thank God for giving me life, knowledge and understanding.

I am grateful to Prof V Sankaran for supervising me; you're indeed a mentor. To me you are a good father.

I am also grateful to:

1. Prof J.E Crafford for reading my proposal;
2. Dr NE Maluta and Mrs. TS Mulaudzi for their help and support.
3. Wife Ndivhuho for her encouragement to start on this project.
4. South African weather services for their useful data.
5. Mr T Ndanduleni and Mr R Makahane for assisting me to set up the experiment for the study.
6. All staff members of physics department for their constant encouragement.

This dissertation is dedicated to the memory of my uncle Joshua Aifheli Nekhubvi.

Abstract

An attempt has been made to test the performance of a solar array under the outdoor condition. Experimental investigations have been made to find its suitability for the rural Limpopo for the small scale electricity generation. This research is also geared towards the testing of validity of the data provided by the manufacture as the commercially available PV modules are rated at standard testing conditions (STC). A 450W ground mounted photovoltaic (PV) system has been designed and installed at the Vuwani Science Resource Centre in Vuwani region, Limpopo Province, South Africa which has geographical coordinates: 23°07'51"S , 30°04'28"E. It is well known that the performance of PV system is dependent on system configuration and weather conditions. The instruments and data acquisition packages have been installed to record some of the main parameters such as peak power and air temperature. The estimated data of solar radiation are used in the present work. The photovoltaic array was connected to the maximum power point tracking (MPPT) charge controller to record daily peak power value produced by the photovoltaic array system. In addition to this, for the testing purposes the DS I-V curve tracer was used to take the electrical current and voltage (I-V) curves of the photovoltaic array installed for normal mode as well as the disturbed mode .The peak power data of the PV system over a period of ten months of operation is recorded, analyzed and the results obtained are discussed. It is noted that the PV system designed and installed is suitable for the chosen location.

CHAPTER-1

RENEWABLE ENERGY TECHNOLOGY

1.1 Introduction

The awareness of renewable energy sources has been extremely limited in our communities. One of the obstacles to the development of renewable energy is the lack of information available to communities about energy. Energy is a critical foundation for economic growth and social progress [1]. Energy can be classified under two broad systems; they are renewable and non-renewable energy [2].The supply of renewable energy is achieved by obliging suppliers to deliver to consumers a portion of their electricity from renewable energy sources [3]. Developing renewable energy, as an appropriate solution of energy bottleneck, is the key to healthy, rapid and sustainable development [4].

Renewable energy is produced by renewable sources such as wind, solar, hydro, geothermal, ocean and biomass [5]. Renewable energies are essential contributors to the energy supply portfolio as they contribute to world energy supply security, reducing dependency on fossil fuel resources, and provide opportunities for mitigating greenhouse gases .Energy is the key issue for most countries, largely in terms of security of supply and costs. Energy is an important input to almost all economic activities; unlike other sectors, production in this sector is not an end in itself. Conceptually, one can define three generations of renewable technologies, reaching more than 100 years. First generation technologies emerged from the industrial revolution at the end of the 19^{th} century and include hydropower, biomass combustion, and geothermal power and heat. Second generation renewable technologies include solar heating and cooling, wind power, modern forms of bio-energy, and solar photovoltaic. Third generations renewable technologies are still under development and include concentrating solar power, ocean energy, enhanced geothermal systems, and integrated bio-energy systems [6].

The use of renewable energy sources is closely linked to sustainable development, because a sustainable supply of energy resources, which must be used effectively and efficiently, is required for it, as well as for progress in environmental problems [7]. While all the renewable

energy sources need to be considered in meeting the energy challenge, solar energy may arguably be the only renewable source capable of supplying a significant fraction of energy at predicted future levels. This is primarily because of the enormous energy resource represented by the sun which continuously floods the earth with 125000TW of power. The solar energy sector has just begun to reveal its enormous potential for growth [8].The present study will focus mainly onto the analysis of the peak power of a photovoltaic solar array system, problem of energy generation, storage and supply in rural resources center at Vuwani region in Limpopo province, South Africa. For this purpose, renewable energy system, represented by second generation renewable technology; silicon solar photovoltaic will be reviewed as a choice for electricity generation.

1.2 Renewable energy technologies

1.2.1 Solar Energy

According to SA year book, (2007/08),Most areas in South Africa average more than 2 500 hours of sunshine per year, and average daily solar-radiation levels range between 4, 5 and 6, 5 kWh/m^2 in one day. The southern African region, and in fact the whole of Africa, is well endowed with sunshine all year round. The annual 24-hour global solar radiation average is about 220 W/m^2 for South Africa compared with about 150 W/m^2 for parts of the United States of America (USA), and about 100 W/m^2 for Europe. This makes the local resource one of the highest in the world. The solar resource is the most readily accessible in South Africa. It lends itself to a number of potential uses. The country's solar-equipment industry is developing. Annual photovoltaic (PV) panel assembly capacity totals 5 MW, and a number of companies in South Africa manufacture solar water heaters. Solar power is increasingly being used for water pumping through the rural water provision and sanitation programme of the Department of Water Affairs.

1.2.2 Solar-passive building design

Research has shown that low-cost housing could be made energy smart by using elementary solar-passive building design practice. This could result in fuel savings of as much as 65%,

which could significantly Energy-efficient homes, may be constructed at the same direct cost (and lower life-cycle cost) as energy-wasteful houses. The challenge is to develop awareness and to ensure implementation of basic energy-efficiency principles. Government is considering the following building norms and standards: orientation for the purposes of passive solar design, lighting, and installation of solar water-heaters, insulation, ventilation, heating and air conditioning [9].

1.2.3 Solar-thermal power generation

The minimum direct normal radiation (DNR) to justify a combined solar-thermal power plant is 1 800 kWh/m^2 per year. According to the Renewable-Energy Resource Database, the area exceeding the minimum required DNR in South Africa covers about 194 000 km^2. A 100-MW solar-thermal plant requires roughly 3 km^2 (1 800 kWh/m^2 per year). If 1% (1 940 km^2) of the identified area is available for solar-thermal power generation, South Africa has an installed potential of 64,6 GW, which is about 36 217 GWh per year. Back-up and energy-storage constraints are limiting the wider economic use of solar-electricity generation (solar thermal and PV) [9].

1.2.4 Solar water heating

The Department of Energy and central energy funds (CEF) have embarked on a solar water-heating project, which promotes the use of solar geysers. The programme targets households, group houses (such as military bases and mine residences) and commercial and industrial applications. Eskom's Solar water-heating programme is an initiative that could lead to a reduction in demand of about 530 MW on the national grid and a favourable contribution to reducing carbon emissions

The mass rollout of SWHs is slow but gaining momentum compared to the commencement of the programme. From April to 31 December 2010, 26 768 rebate-funded SWHs have been installed whilst about 30 974 systems have been installed since the advent of the programme in November 2008. These figures are spread across the country. Notwithstanding these lower than desired installation figures, the 2014 target is still in sight. The illustration below shows the healthy growth seen in the national SWH programme up to end October 2010[10].

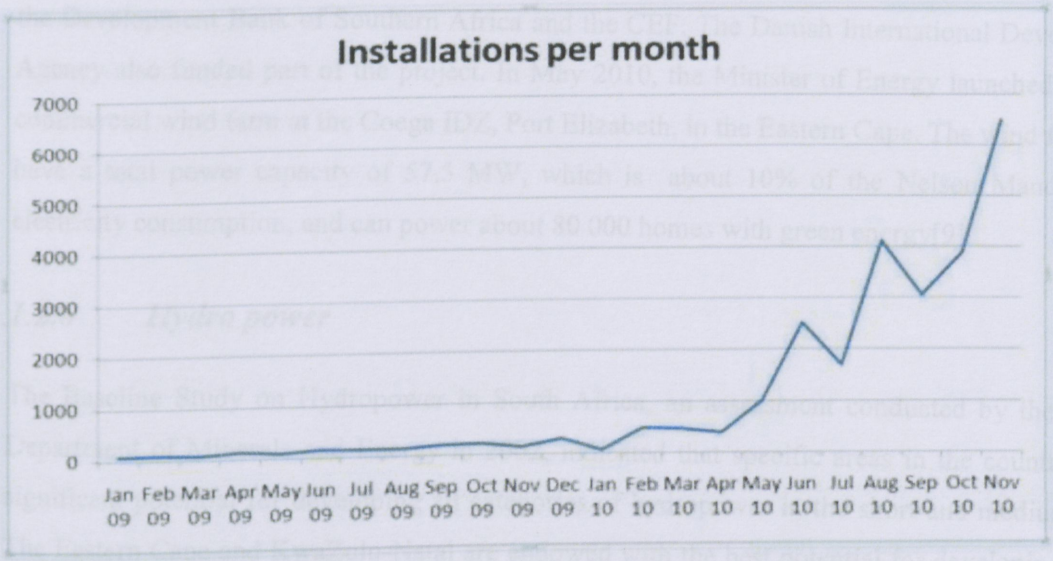

Figure 1.1 The healthy growth seen in the national SWH programme up to end October 2010 [Source: South African energy synopsis, 2010]

1.2.5 Wind energy

As mentioned in SA year book (2007/08) Eskom's Klipheuwel, just north of Cape Town, is the first large wind-turbine facility in sub-Saharan Africa. The pilot phase of the Klipheuwel research and demonstration project ran from 2002 to 2005. During that time, the Klipheuwel Pilot Wind Farm generated more than 12 GWh of electricity, reducing carbon-dioxide emissions by 11 000 t. The three wind turbines operated at an average availability of 90%. The project's research phase has been completed and the wind farm will be operated commercially for its anticipated 20-year lifespan as calculated from 2006. The R75-million national demonstration project in Darling in the Western Cape was the first "green-energy" initiative in the country to produce electricity from wind power on a commercial basis. The Darling Wind Farm has four wind turbines, which can supply 5, 2 MW. All the electricity produced would be sold to the City of Cape Town as part of a long-term power agreement with the city. The facility consists of four German-designed wind turbines. The structures are 50 m high with the blades spanning 31 m. Each turbine will produce 1,3 MW, bringing the total output of the wind farm to 5,2 MW. The project is referred to as the National Demonstration Project and will be used as an example for future public-private partnerships in the establishment of alternative electricity generation. The project was developed through collaboration between the Darling Independent Power Producer,

the Development Bank of Southern Africa and the CEF. The Danish International Development Agency also funded part of the project. In May 2010, the Minister of Energy launched the first commercial wind farm at the Coega IDZ, Port Elizabeth, in the Eastern Cape. The wind farm will have a total power capacity of 57,5 MW, which is about 10% of the Nelson Mandela Bay electricity consumption, and can power about 80 000 homes with green energy[9].

1.2.6 Hydro power

The Baseline Study on Hydropower in South Africa, an assessment conducted by the former Department of Minerals and Energy in 2002, indicated that specific areas in the country show significant potential for developing all categories of hydropower in the short and medium term. The Eastern Cape and KwaZulu-Natal are endowed with the best potential for developing small, that is, less than 10 MW hydropower plants. The advantages of these plants are that they can either be stand-alone or exist in a hybrid combination with other renewable energy sources. Advantage can be derived from the association with other uses of water (such as water supply, irrigation and flood control), which are critical to the future economic and socio-economic development of South Africa. Eskom has started the construction of the Ingula Pumped Storage Scheme (1 332 MW) near Van Reenen, KwaZulu- Natal. It is expected that the first unit will be operational in 2013[9].

1.2.7 Biomass

Biomass is estimated to contribute about 10% of South Africa's primary energy. Biomass can be divided into wood and bagasse.

1.2.7.1 Wood

Wood as a source of energy in South Africa has two quite different uses, industrial and domestic. The industrial use is by South Africa's modern pulp and paper industry, which has a production of about 4.5 Mt a year. In the chemical pulp mills, the fibre is separated out in chemical digesters and the residue, known as "black liquor" and containing useful energy, is burned in recovery boilers to raise steam for process heat and electricity generation. Bark and sawdust from the wood is also burned in boilers.

The domestic use is by poor households, mainly in the remote un-electrified rural areas. Wood is a very important residential fuel in South Africa, as it is throughout the continent. It is used for domestic purposes including cooking, heating water, space heating and others. The exact amount of residential wood fuel used is unknown but estimates put is at 86 PJ/yr. roughly equivalent to 7Mt of wood per year.

1.2.7.2 Bagasse

Bagasse, the waste fibre from sugar cane, is the most important energy source for South Africa's sugar refining industry. The total sugar cane crop is over 20 Mt a year, which yields about 7 Mt of bagasse with a heating value of 6.7 MJ/kg, most of which is used as energy in raising steam for process heat and electricity generation. The installed generation capacity of the industry is about 245 MW.

1.2.8 Ocean energy

Ocean energy could potentially be derived from the various characteristics of the sea. For example, the rise and fall of the waves could be converted into hydraulic pressure by mechanical compression devices. Such pressure could drive a turbine generator to produce electricity, while the tidal variation, sea current and different thermal layers in the ocean could also be used. The main reason why this energy resource is not currently being harnessed is that no reliable technology exists that can generate electricity from this resource. Various companies are testing systems internationally to develop technically viable solutions. Once technical reliability has been proven, cost-effectiveness in relation to other solutions will have to be established. Eskom continues with resource surveys of the Agulhas Current on the east coast of South Africa and of wave energy, in partnership with the Department of Environmental Affairs and the Bay world Centre for Research and Education. Results have proved the technical feasibility of extracting significant large-scale renewable energy from the current [9].

1.3 South African energy (electricity) generation, supply and access

Electricity, as a key strategic economic sector, underpins government's growth and development objectives. Electricity is different from other services we find in homes, unlike air, water that can

be harvested from nature, electricity must be manufactured. Much of the world has seemingly settled into fossil fuels as though they will be forever available. South Africa relies heavily on coal to meet its energy needs because it is well-endowed with coal resources; in particular, South Africa has developed an efficient, large-scale, coal-based power generation system that provides low-cost electricity, through a grid system that is being extended to rural areas, to millions of residential, commercial and institutional consumers.

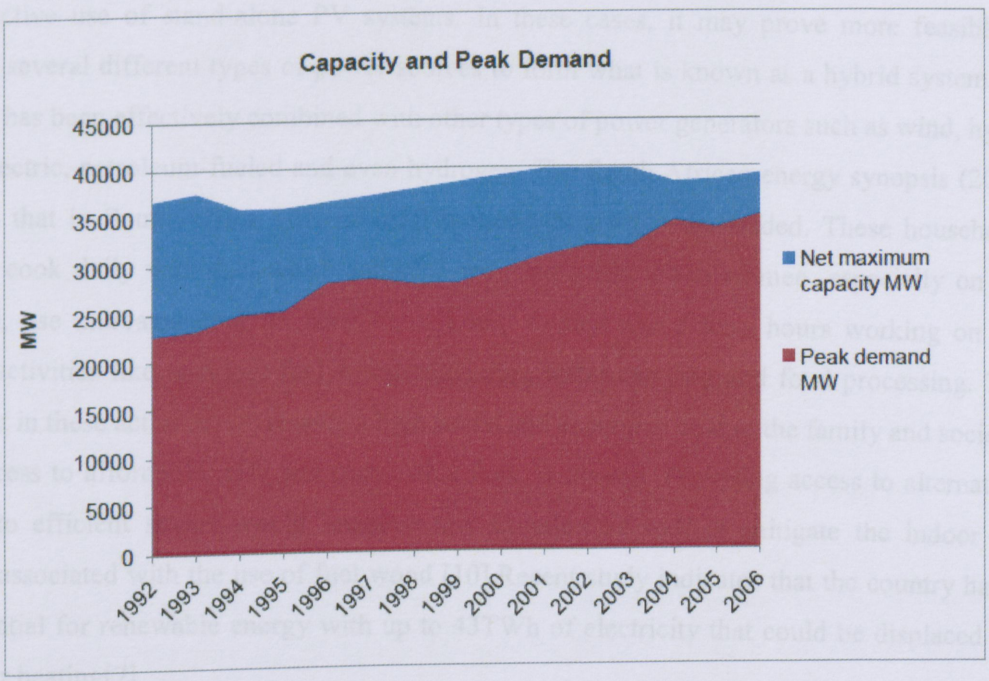

Figure1.2 Electricity generation capacity versus peak electrical demand (DoE, 2009b:44)

As a result, coal is and is likely to remain, from a financial viewpoint, an attractive source of energy for South Africa. However, at the same time South Africa recognizes that the emissions of greenhouse gases, such as carbon dioxide, concerns worldwide, about global climate change. While South Africa is well endowed with renewable energy resources that can be sustainable alternatives to fossil fuels, so far these have remained largely untapped [11].

Using coal to generate electricity is not ideal because, no matter how carefully it is burnt: there are gaseous and solid emissions. The gases that are given off include sulphur dioxide, carbon dioxide and oxides of nitrogen, the first two of which are regarded as having climate-change

effects on the environment [9].The graph in figure 1.1 shows how the peak demand of energy changes overtime. The peak demand increased almost every year. This is the results of the fast growing population of South Africa. Many households and factories are being built in all parts of South Africa.

Electrical energy requirements for many remote areas in South Africa are too large to allow the cost-effective use of stand-alone PV systems. In these cases, it may prove more feasible to combine several different types of power sources to form what is known as a hybrid system. To date, PV has been effectively combined with other types of power generators such as wind, hydro thermoelectric, petroleum-fueled and even hydrogen. The South African energy synopsis (2010) indicated that in South Africa 80% of rural households are female-headed. These households typically cook daily with fuel-wood and crop residues while urban women, especially on the high-veld, use untreated coal. In rural households, women spend long hours working on the survival activities like cooking, fuel wood collection, water carrying and food processing. The time spent in these activities represents a high social and economic cost to the family and society, where access to affordable, safe and sustainable fuels is limited. Providing access to alternative fuels or to efficient stoves would improve this situation as well as mitigate the indoor air pollution associated with the use of fuel wood [10].Recent study indicates that the country has a high potential for renewable energy with up to 43TWh of electricity that could be displaced by solar water heating[7].

Electricity supply is one of the most important utilities that underpin the survival of a nation's critical infrastructures and services such as natural gas supply, water supply services, transportation, telecommunications, financial services and healthcare services. South Africa supply two thirds of electricity and is one of the four cheapest electricity producers in the world [11]. Since 1994 several energy projects were set up in South Africa to provide remote rural communities with electricity supply through PV systems [12].The figure depicted below shows the primary energy supply for 2006 in South Africa. From the figure 1.2 one can clearly observe that coal was still leading followed by crude oil. The renewable technology is also growing as seen from the figure1.2.

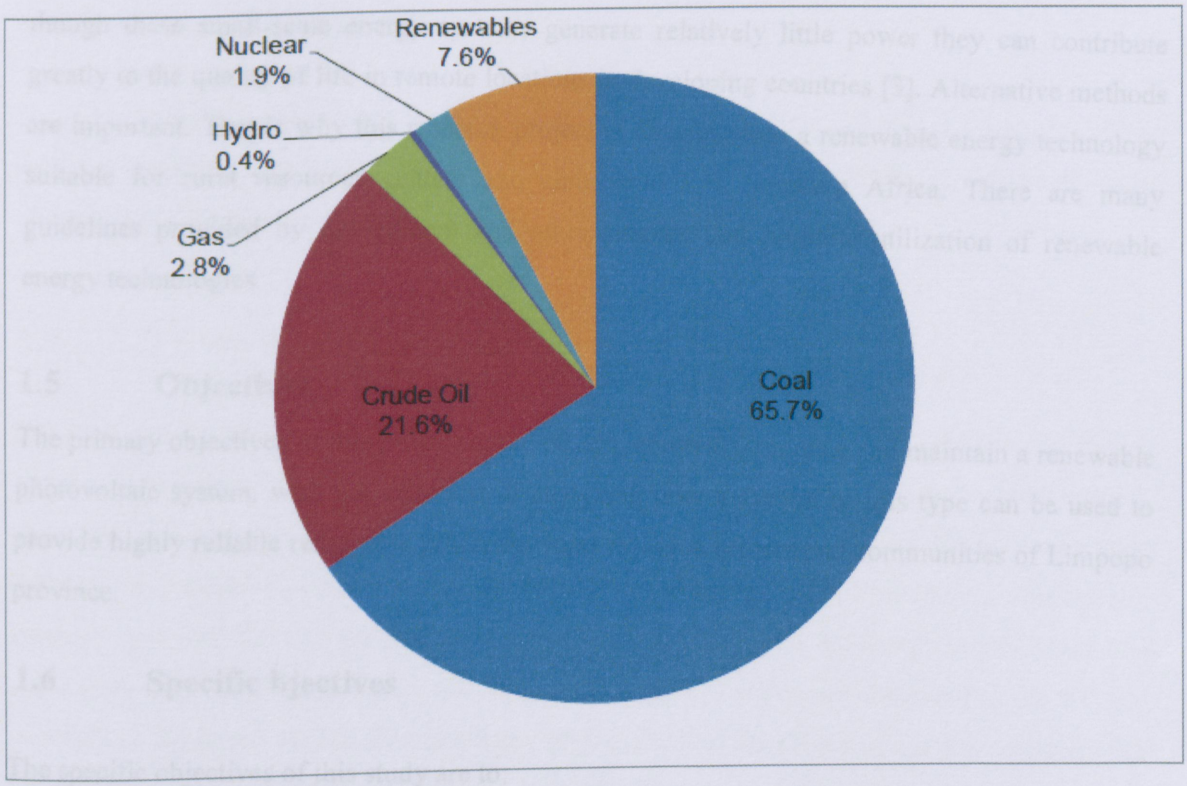

Figure 1.3 Primary energy supply for 2006, total: 5560 PJ (DME, 2009)

In his state of the nation address, the former President Thabo Mbeki announced the target of universal access to electricity for all South Africans by 2012 [12]. In South Africa access to electricity increased from 35% of households in 1990 to 84% in 2011 [13].

1.4 Rationale for the study

The Government has brought electricity to both urban and rural areas and this has resulted in an improvement in the quality of lives of our people [10]. Connecting homes and resources centers to the country's electricity grid is very expensive in South Africa especially as we get deeper and deeper into the rural areas. In many cases, grid extension is impractical because of dispersed populations, rugged terrain, or both. Thus, small off-grid stand- alone renewable energy systems represent an important option for narrowing the electricity gap in rural parts of the developing world, where progress in grid extension remains slower than population growth [1,2]. Even

though these small-scale energy systems generate relatively little power they can contribute greatly to the quality of life in remote locations in developing countries [3]. Alternative methods are important. That is why this research project is focusing into a renewable energy technology suitable for rural resources centers and communities of southern Africa. There are many guidelines provided by government and other sources that promote utilization of renewable energy technologies.

1.5 Objectives

The primary objectives of this project are to design, construct, monitor and maintain a renewable photovoltaic system, with the intention of analyzing how a system of this type can be used to provide highly reliable renewable power for rural resource centers and communities of Limpopo province.

1.6 Specific bjectives

The specific objectives of this study are to:

- Install a small photovoltaic power system.
- Determination of amount solar radiation that falls in Vuwani region with a view to estimate the amount of solar energy that can be used in the area as a way of harnessing solar radiation through renewable energy technology.
- Analyze the peak power of an installed photovoltaic solar array.

1.7 Key questions

The research is geared towards providing the solar energy end-user, as well as those concerned with the installation of solar energy systems, with information on the insolation in Vuwani area.

The following are questions that the research project attempts to solve:

1. How much solar energy reaches Vuwani region each year?
2. How much solar energy can be used to generate electrical energy in Vuwani region?

1.8 Beneficiaries

People who will benefit from this work are solar energy researchers, schools, clinics, post offices and farms and rural communities around Limpopo province and elsewhere in the country since these people will be able to use some of the measured and estimated data.

1.9 Energy from the sun

The energy from the sun can be used directly to heat or light buildings, and to heat water, in both developed and developing nations. The sun's radiant energy can also directly provide very hot water or steam for industrial processes, heat fluids through concentration to temperature sufficient to produce electricity in thermal-electric generators or to run heat engines directly, and produce electricity through the photovoltaic effect [14].Where does the energy output of the Sun come from? Our sun is an ordinary star, average in size and brightness, compared to the millions of others in the universe. The Sun is a huge, glowing ball at the center of our solar system. The sun provides light, heat, and other energies to Earth. The sun is made up entirely of gas. Most of it is a type of gas that is sensitive to magnetism. This sensitivity makes this type of gas so special that scientists sometimes give it a special name: plasma [15].

CHAPTER-2

METEOROLOGICAL PARAMETERS AND PHYSICS OF SEMICONDUCTORS

2.1 Solar radiation

The various fluxes of radiation to and from the earth's surface are amongst the most important variables in the heat economy of the earth as a whole and either at any individual place at the earth's surface or in the atmosphere. Radiation quantities may be classified into two groups according to origin: solar global radiation and terrestrial radiation. Solar radiation is the energy emitted by the Sun. The solar radiation incident on the top of the terrestrial atmosphere is called extra-terrestrial solar radiation; that 97% of it that is confined to the spectral range 0.29 to 3.0 μm is called Short-wave radiation. Part of the extraterrestrial solar radiation penetrates through the atmosphere to the earth's surface, while part of it is scattered and/or absorbed by the gas molecules, aerosol particles, cloud droplets, and cloud crystals in the atmosphere. Terrestrial radiation is the long-wave electromagnetic energy emitted by the earth's surface and by the gases, aerosols, and clouds of the atmosphere; it is also partly absorbed within the atmosphere [16].In the present work solar radiation measurements are used for the study of the transformation of energy within the earth-atmosphere system and of its variation in time and space

2.2 Solar Radiation Measurements

The solar radiation received from a solid angle of 2π steradian on a horizontal surface is referred to as global radiation. These include radiation received directly from the solid angle of the Sun's disk, as well as diffuse sky radiation that has been scattered in traversing the atmosphere.

The instrument needed for measuring solar radiation from a solid angle of 2πsteradians into a plane surface and a spectral range from 0.3 to 3.0 mm is the pyranometer. The pyranometer is sometimes used to measure solar radiation on surfaces inclined in the horizontal and in the inverted position to measure reflected global radiation.

When measuring the diffuse component of solar radiation alone, the direct solar component may be screened from the pyranometer by a masking device. Pyranometers normally use thermoelectric, photoelectric, pyroelectric, or bimetallic elements as sensors. Since pyranometers are exposed continually in all weather conditions they must be robust in design and resist the corrosive effects of humid air (especially near the sea). The receiver should be hermetically sealed inside its casing or the casing must be easily removable so that any condensed moisture can be removed. Where the receiver is not permanently sealed, desiccators are usually fitted in the base of the instrument. The properties of pyranometers that are of concern when evaluating the uncertainty and quality of radiation measurement are: sensitivity, stability, response time, cosine response, azimuth response, linearity, temperature response, and spectral response [16].

Thermopile instruments exhibit changes in sensitivity with variations in instrument temperature. Some instruments are equipped with built-in temperature compensation circuits in an effort to maintain a constant response over a large range of temperatures. The temperature coefficient of sensitivity may be measured in a temperature-controlled chamber. The temperature in the chamber is varied over a suitable range (–40 to 40°C) in 10° steps, and held steady at each step until the response of the pyranometers has stabilized. The data are then plotted and a smooth curve drawn through the points. If the maximum percentage error due to temperature response is two per cent or more, a correction should be applied on the basis of the best straight-line fit of the data over the temperature range of interest. If no temperature chamber is available, then the standardization method with pyrheliometers can be used at different ambient temperatures. Attention should be paid to the fact that not only the temperature, but also, for example, the cosine response (i.e. the effect of solar elevation) and the nonlinearity (i.e. variations of solar irradiance) can change the sensitivity [16].

2.3 Solar Radiation Distribution in Southern Africa

South Africa experiences some of the highest levels of solar radiation in the World [10]. The average daily solar radiation in South Africa varies between 4.5 and 6.5 kWh/m^2 (16 and 23 MJ/m^2) compared to about 3.6 kWh/m^2 for parts of the United States and about 2, 5 kWh/m^2 for parts of Europe and the United Kingdom [9].

2.4 Daily beam and diffuse components of solar irradiance from the monthly daily average of total irradiance on a horizontal surface

In order to estimate the solar energy that can be collected by a flat plate solar collector, it is necessary to know the total of the incident radiation. Knowing the total daily insolation on a horizontal surface, it is possible to estimate the beam and the diffuse solar radiation incident on the collector during the day. It has been found that the long term average ratio of the diffuse radiation to the total hemispherical radiation on a horizontal surface, H_d/H_h, is strongly dependent on the sunset hour angle, w_s, and the clearness index k_h. Periera and Rabl [17] found that the ratio H_d/H_hcan be expressed as:

$$\frac{H_d}{H_h}=a\text{-}bc \tag{2.1}$$

where,

$$a = 0.775 + 0.00606(\omega_s - 90)$$

$$b=0.505+0.00456(\omega_s-90)$$

$$c = \cos(115k_h - 103)$$

And the clearness index K_h is defined as the ratio between the total irradiance on a horizontal surface H_h and the extraterrestrial insolation H_o

$$K_h = \frac{H_h}{Ho} \tag{2.2}$$

For a certain period of time K_h is:

$$K_h=\frac{1}{N}\sum_{i=1}^{N}\frac{H_{h(i)}}{H_{0(i)}} \tag{2.3}$$

Once H_d has been found, the long term beam component can be found according to the relation:

$$H_b = H_h - H_d$$

2.5 Hourly total irradiance on a horizontal plane

The hourly solar radiation on a horizontal surface is found to be dependent on the sunset hour angle. The ratio of hourly total to daily total solar radiation is given by:

$$\frac{I_{tot}}{H_h} = \frac{\pi}{24}(A+B\cos\omega)\left[\frac{\cos\omega-\cos\omega_S}{\sin\omega_S-(2\pi\omega_S/360)\cos\omega_S}\right] \quad (2.4)$$

where, I_{tot} is the hourly total radiation on horizontal surface in mega Joule per meter square. The coefficient A and B are given by:

$$A = 0.409 + 0.5016\sin(\omega_S - 60)$$

$$B = 0.6609 - 0.4767\sin(\omega_S - 60)$$

2.6 Hourly beam and diffuse radiation components on a horizontal plane

The ratio of hourly diffuse to daily diffuse solar radiation I_d/H_d had been developed by Liu and Jordan in 1960[17] .this ratio is given by

$$\frac{I_d}{H_d} = \frac{\pi}{24}\left[\frac{\cos\omega-\cos\omega_S}{\sin\omega_S-(2\pi\omega_S/360)\cos\omega_S}\right] \quad (2.5)$$

Where, I_d and H_d are the hourly and the daily diffuse solar radiation on horizontal surface respectively in MJ/m^2.the hourly beam component can be easily estimated according to the expression:

$$I_b = I_t - I_d \quad (2.6)$$

2.7 Hourly beam and diffuse radiation components on an inclined plane

In general, any plane oriented towards the sun is making an angle with the incident solar beam. This angle, between the solar beam and the normal to the surface is called the angle of incident θ_i and can be expressed as:

$$\cos\theta_i = \sin\delta\sin\phi\cos\beta - \sin\delta\cos\phi\sin\beta\cos\gamma + \cos\delta\cos\phi\cos\beta\cos\omega + \cos\delta\sin\phi\sin\beta\cos\omega\cos\gamma + \cos\delta\sin\beta\sin\omega\sin\gamma \quad (2.7)$$

where :

δ =declination angle

β =tilt angle

ϕ =latitude angle

γ =the angle by which the collector is diverted from the south

In most of the applications where the solar collectors are maintained fixed, the collectors are sloped towards the equator, in this case $\gamma = 0^o$ and the expression for θ_i is simplified to be:

$$\cos\theta_i = \cos(\phi-\beta)\cos\delta\cos\omega + \sin(\phi-\beta)\sin\delta \quad (2.8)$$

It can be noticed that this incident angle is equivalent to the azimuth angle of locality ϕ' latitude such that, $\phi' = \phi - \beta$.

Defining R_b as the ratio of beam radiation on tilted plane to a horizontal plane then:

$$R_b = \frac{I_{bT}}{I_b} = \frac{\cos\theta_i}{\cos\theta_z} \quad (2.9)$$

where θ_z is zenith angle and is given by the expression:

$$\cos\theta_Z = \cos\delta\cos\phi\cos\omega + \sin\phi\sin\delta \quad (2.10)$$

The diffuse radiation on tilted surface is composed of two components. They are diffuse solar radiation from hemisphere I_{dh} and solar radiation diffusely reflected from the ground I_{dg}. The expressions for I_{dh} and I_{dg} are given by

$$I_{dh}=I_d\frac{1+\cos\beta}{2} \tag{2.11}$$

and

$$I_{dg}=I_{tot}\rho g\frac{1-\cos\beta}{2} \tag{2.12}$$

where $(1+\cos\beta)/2$ is known as the view factor of the tilted surface to the sky and ρ_g is the reflectivity of the surroundings. The factor $(1-\cos\beta)/2$ is known as the surface view factor to the ground. The total diffuse radiation on tilted surface I_{Dt} can be simply estimated by adding the two diffuse components,

$$I_{dT}=I_{dh}-I_{dg} \tag{2.13}$$

Solar radiation and the position of the panel with regard to the incoming radiation play an important role in providing the efficiency as well as increasing the energy which can be harnessed from the sun [17].

2.8 Air temperature

Temperature is defined as a physical quantity characterizing the mean random motion of molecules in a physical body. Temperature is characterized by the behaviour that two bodies in thermal contact tend to an equal temperature. Thus temperature represents the thermodynamic state of a body and its value is determined by the direction of the net flow of heat between two bodies. In such a system, that body which overall loses heat to the other is said to be at the higher temperature. The most common variable that is measured is air temperature at various heights. Other variables are ground, soil and seawater temperature. World Meteorological Organization defines air temperature as the temperature indicated by a thermometer exposed to the air in a place sheltered from direct solar radiation [16].The photovoltaic I-V curve characteristic is measured at the determined nominal operating cell temperature (NOCT) and an irradiance of 800W/m^2. After excluding data recorded when the wind is too strong or the ambient temperature

not sufficiently stable, the temperature rise of the module above the ambient temperature (T_J-T_{amb}) is ploted against irradiance and best fit line drawn through the points. The interpolated value of (T_J - T_{amb}) at 800W/m^2 is then added to 20°C to give the NOCT [17].

2.9 Theoretical consideration of Photovoltaics

The basic property of semiconductors, which makes them suitable for photovoltaic applications, is their band structure. The valence band of any semiconductor is fully occupied at low temperatures, while the conduction band is empty. However, at room temperature the thermal motion of electrons can excite some electrons to conduction band. The probability of occupation of energy state is given by Fermi-Dirac distribution

$$f(E) = \frac{1}{1+e^{\left(\frac{E-E_F}{KT}\right)}} \tag{2.14}$$

Where $f(E)$ is the occupation probability, E_F is the Fermi-level energy, K is the Boltzmann constant and T is the temperature. The density of state for electrons in the conduction band and holes in the valence band $g_e(E)$, can be written as;

$$\left(g_e(E)\right)=8\sqrt{2}\pi m^{\frac{3}{2}}{}_e(E-E_c)^{\frac{3}{2}}\,dE \tag{2.15}$$

And

$$\left(g_h(E)\right)=8\sqrt{2}\pi m^{\frac{3}{2}}{}_e(E_v-E)^{\frac{3}{2}}\,dE \tag{2.16}$$

where E_v and E_c are the conduction band energy and the valence band energy respectively. And m_e and m_h are the effective masses of electrons in the conduction band and holes in the valence band respectively. With the help of the two equations above, an equation can be derived for the density of electron in the conduction band and in a simplified form this equation can be written as ;

$$n = N_c e^{\left(\frac{E_f-E_c}{KT}\right)} \tag{2.17}$$

and the density of holes in valence band, p , is

$$p = N_v e^{\left(\frac{E_v-E_f}{KT}\right)} \tag{2.18}$$

where N_c and N_v are the effective density of state in the conduction band and valence band respectively. The above equations are both valid for pure and doped semiconductor, even though the Fermi level is shifted in the latter.

2.10 Effective masses in semiconductors

In many semiconductors it has been possible to determine by cyclotron resonance the form of the energy surfaces of the conduction and valence bands near the band edges. The determination of the energy surface is equivalent to a determination of the effective mass tensor:

$$\left(\frac{1}{m^*}\right)_{\mu\nu} = \frac{1}{\hbar^2}\frac{d^2\varepsilon}{dk_\mu dk\nu}; \tag{2.19}$$

$$\frac{dv_\mu}{dt} = \left(\frac{1}{m^*}\right)_{\mu\nu} F_\nu \tag{2.20}$$

where μ and ν are Cartesian coordinates

Photovoltaic cell requires a material where photons can excite electrons to an exited state. The device needs an internal electric field to separate the excited carriers and ohmic connections to deliver the power to a load. A semiconductor with a *p-n*-junction can perform these functions. The number of known semiconductors that can be used as solar cell material is not as large as one would anticipate [18].

2.11 Photovoltaic solar cell materials

2.11.1 Crystalline silicon

Most PV modules being shipped today are single crystal, multi crystalline, or ribbon based solar cells. Research and development in this area has taken advantage of the wealth of knowledge developed for silicon integrated circuit manufacturing and developed structures that maximize the electron hole generation and reduce surface and bulk recombination. Another important research activity dealing with silicon based cells is how to close the differences between the less perfect materials, namely multi crystalline and ribbon silicon, and single crystal cells. The development of plasma and other nitriding processes by the semiconductor electronics industry

has led to improvements in single and multi-crystalline silicon cells and ribbon silicon cells in particular[8].

Crystalline silicon solar cells respond very rapidly to sudden changes of irradiance, their time constant being about 20uS.an increase in temperature causes a slight rise in the short circuit current but a sharp fall in open circuit voltage and maximum power. Because of the loss of power with increasing temperature, it is important module and system design to ensure that the cells run as coolly as possible [19].

2.11.2 Thin film

Thin film PV technologies are now entering the world commercial market. Although their market share is still very small, growth is rapid, driven in part by capacity problems with crystalline silicon. Research results with these systems have been very impressive with laboratory device efficiencies for some systems approaching 20%.despite the very positive potential of these technologies, there is a strong need for basic research to better understand fundamental properties of these materials and devices, especially of interfaces ,new multijunction designs, low cost, high performance transparent conductor oxide materials, alternative module concepts, and of methods for increasing device and module efficiencies[8]. Amorphous silicon (a-Si) is the best developed thin film material and has been in commercial production since 1980, initially for use in hand held calculators.

The amorphous nature has several important consequences for photovoltaics. Absorption of visible light is better than for crystalline silicon, but doping and charge transport are more difficult. Amorphous silicon suffers from light-induced degradation known as the Staebler Wronski effect the defect density in a-Si:H increases with light exposure, over a time scale of months, to cause an increase in the recombination current and reduction in efficiency. It is believed that light energy breaks some GaSi:H bonds to increase the density of dangling bonds. The system is excited into a higher energy centigrade allows the structure to relax, and the dangling bonds to be re-saturated .for this reason a-Si:H solar cells may perform rather better in high temperatures environments. In typical a- Si solar cells the efficiency is reduced by up to 30% in the first six months as a result of the Staebler Wronski effect, and the fill factor falls over

0.7 to about 0.6. This light induced degradation is the major disadvantage of a-Si as a photovoltaic material. The availability of alloys with different band gap enables the design of hetero-structure and tandem devices [20].

2.11.3 Multijunction Tandem cells

The multi-junction cell approach is the most mature and most successful third generation technique for improving performance over a single-junction cell. Here solar cells are stacked in order of their band gap, with solar radiation entering the largest band gap cell first. Light is automatically filtered as it passes through the stack, with each cell absorbing a narrow energy range of above band gap photons, thereby minimizing hot carrier losses. Below band gap photons are transmitted and those with energies above the smallest band gap in the stack have a high probability of being absorbed, minimizing below band gap losses. The result is the multijunction solar cell with an ideal efficiency determined by the number of cells in series. the theoretical efficiency limit is 86.8% for an infinite number of band gap energies at very high solar concentration levels. If band gaps are appropriately selected so that each cell in the stack generates nearly the same current, the cells can be interconnected in series making monolithic integration possible. A multi-junction thin film approach that is now in volume manufacturing utilizes hydrogenated amorphous silicon (a-Si:H) and silicon [8].

2.12 Photovoltaic market

By 2050 world energy consumption is predicted to grow from the present 13 TWyr to 30 TWyr. To meet this huge demand, the global energy sector will be facing two main pressing issues, (i) declining fossil reserves and (ii) climate change due to man- made greenhouse emissions. Generating a dramatic increase in PV –produced power is a significant challenge. Present PV production is almost insignificant relative to fossil fuel generation and cost, which is presently almost 10 times higher than coal produced electricity, is the key issue. At the same time, PV manufacturing is growing exponentially, at approximately 30% per year and this rate is, if anything, increasingly. The impressive progress is also due to the substantial technology improvements in material quality, devices processing, fabrication and design, and also in

characterizations. All these together led to better device performance and reliability, and lowered the systems costs [8].

2.13 Photovoltaic solar array

Packaged solar modules are very easy to install. They are designed for outdoor use with no additional protection, so all that is needed is a rigid support that will not sway in the wind or collapse under snow. Large arrays can be mounted directly onto a roof or they can even be part of the roof structure. Because of their ability to operate for years without any attention, solar cells can be permanently installed in sorts of creative ways: onto a car roof to trickle charge the battery whenever the car is parked in the sun; as canopies or sun shades on golf carts to extend their range; on the entire top wing of a glider to run a small prop. In a permanent installation, it is important to orient the solar cell array so that it makes the most effective use of available sunlight. If the array is to be fixed in place, the most useful general orientation is facing due south and tilted at an angle from the vertical equal to the latitude.

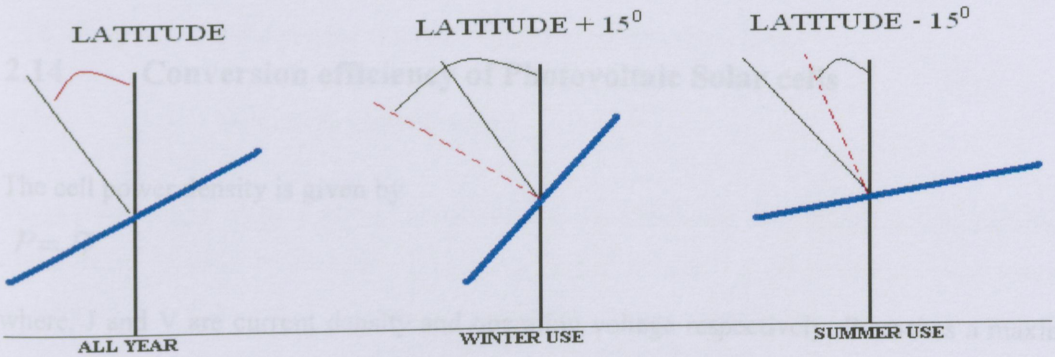

Figure 2.1 Suggested tilt angle for the three situations

If the array is to be used in winter, or if that is when the short days and cloudy weather put the greatest strain on the system to meet load requirement, the array can be tilted down a maximum of 15^0 to increase its efficiency. Presumably the loss in efficiency that this would cause in summer is more than made up for by the increased amount of sunlight. if the system is used only in summer ,it could be tilted up additional 15^0 from the latitude. The changes in angle only change the overall efficiency by about 5% the figure above shows the suggested tilt angle for the three situations [19].The dotted lines shows that the tilt angle is changing during winter, summer as well as all year.

When charged by the sun, this basic unit generates a dc photovoltage of 0.5 to 1 volt and, in short circuit, a photocurrent of some tens of milliamps per cm^2. Although the current is reasonable, the voltage is too small for most applications. To produce useful dc voltages, the cells are connected together in series and encapsulated into modules. A module typically contains 28 to 36 cells in series, to generate a dc output voltage of 12V in standard illumination conditions. The 12V modules can be used singly, or connected in parallel and series into an array with a large current and voltage output, according to the power demanded by the application. Cells within a module are integrated with bypass and blocking diodes in order to avoid the complete loss of power which would result if one cell in the series failed. Modules within arrays are similarly protected. The array, which is also called a photovoltaic generator, is designed to generate power at a certain current and a voltage which is some multiple of 12V, under standard illumination. Photovoltaic systems engineering depends to a large degree upon the electrical characteristics of the individual cells [8].

2.14 Conversion efficiency of Photovoltaic Solar cells

The cell power density is given by

$$P=JV \tag{2.21}$$

where, J and V are current density and operating voltage respectively. P reaches a maximum at the cell's operating point or maximum power point. This occurs at some voltage Vm with a corresponding current density Jm at maximum power point, the optimum load thus has shunt resistance given by Vm/Jm. The efficiency η of the cell is the power density delivered at operating point as a fraction of the incident light power density, Ps.

$$\eta=\frac{J_m V_m}{P_S} \tag{2.22}$$

Efficiency is related to J_{sc} and V_{oc} using FF

$$\eta=\frac{J_{sc} V_{oc} FF}{P_S} \tag{2.23}$$

These four quantities: η , *Jsc*, *Voc and FF* are the key performance characteristics of a solar cells.All of these should be defined for particular illumination conditions. The Standard Test Conditions (STC) for solar cells is the Air Mass 1.5, an incident power density of 1000W/m^{2}and temperature of 25^{0}C [20].

2.15 PV system azimuth and slope

The azimuth is the direction towards which the PV panels face. Due south is 0°, due east is -90°, due west is 90°, and due north is 180°. With fixed-azimuth systems, the panels are almost always oriented towards the equator (0° azimuth in the northern hemisphere, 180° azimuth in the southern hemisphere). The azimuth is insignificant if the panels are mounted horizontally (zero slope). The slope is the angle at which the panels are mounted relative to the horizontal. A slope of 0° corresponds to horizontal, and 90° corresponds to vertical. With fixed-slope systems, a slope roughly equal to the latitude will typically maximize the annual PV energy production. The azimuth specifies the direction towards which the panels slope [21].

2.16 I-V Curves Normalization

Since photovoltaic system performance depends on irradiance and operating temperature, curve normalizing is used to translate I-V curves taken at one set of irradiance and temperature conditions to a different set of irradiance and temperature conditions. This is done so that I-V curves taken under different conditions can be compared as if they were taken under identical conditions. Usually curves are normalized to standard testing conditions of irradiance at 1000 W/m^2 and temperatures of either 25°C 45°C. It is important to understand that any form of normalization is only an approximation and that significant errors will occur if I-V curves are normalized over large ranges of irradiance or temperature. The accuracy of the normalization depends on the technique and the unique characteristics of the PV system [22].

2.17 Normalizing techniques

There are three normalizing techniques that are employed by the IVPC to normalize the I-V curves namely;

2.17.1 Approximation technique

The approximation technique is a simple technique useful when exact normalization coefficients are unknown. This technique does not adjust current for temperature changes, but can correct voltage for temperature. The recommended voltage correction for temperature (β) is best left at negative 0.5% (-0.005). This is the default value used by IVPC. This approximation normalization technique uses the following equations to translate an I-V curve from actual conditions to the normalized conditions [22].

$$I_0 = I + I_{sc}\left(E_0/E - 1\right) \tag{2.30}$$

$$V_0 = V + \beta V_{oc}\left(T_0 - T\right) - R_s I_{sc}\left(E_0/E - 1\right) \tag{2.31}$$

where,

I_o = Normalized current value

V_o = Normalized voltage value

E_o= Normalized Irradiance (typically 1000 W/m^2)

T_o = Normalized temperature (often 25°C or 45°C) I = Original current value

V = Original voltage value

E = Original Irradiance

T = Original temperature

R_s = IV curve series resistance , β = Voltage temperature correction (1/°C)

2.17.2 ASTM E technique of 1036 1993

This normalization technique adds the Alpha (α) correction of current for temperature changes. It also includes a correction based on the series resistance of the IV curve. If the series resistance is

unknown, IVPC can estimate the series resistance using the slope of the IV curve as it approaches open-circuit voltage. This normalization also includes a curve correction factor. This normalization technique uses the following equations to translate an IV curve from actual conditions to the normalized conditions [22].

$$I_o = I + \Delta I \tag{2.32}$$

$$V_o = V + \beta\left(T_o - T\right) - \Delta I\ R_s - K\ I_o\left(T_o - T\right) \tag{2.33}$$

$$\Delta I = I\left[\left(E_o / E - 1\right) + \alpha\left(T_o - T\right)\right] \tag{2.34}$$

Where K and α, are the Curve Correction Factor (Ohms/°C) and Current temperature correction (1/°C) respectively.

2.17.3 *ASTM E technique of 1036-1996*

This normalization technique is more or less the same as the ASTM E 1036 1993 since this technique adds more correction coefficients. This normalization technique uses the following equations to translate an IV curve from actual conditions to the normalized conditions [22].

$$I_o = I\left(E_o / E\right) / \left(1 + \alpha_E\ T - \alpha_{E_o}\ To\right) \tag{2.35}$$

$$V_o = V / \left[\left(1 + \beta_E\ T - \alpha_{E_o}\ To\right)\left(1 + \Delta T\ ln\left(E\right) - \Delta T_o\ ln\left(E_o\right)\right)\right] \tag{2.36}$$

α_E = Current temperature correction at irradiance E (1/°C)

α_{E_o} = Current temperature correction at irradiance E_o (1/°C)

β_E = Voltage temperature correction at irradiance E (1/°C)

β_{E_o} = Voltage temperature correction at irradiance E_o (1/°C)

ΔT = Voltage-Irradiance correction factor at T (no units)

ΔT_o = Voltage-Irradiance correction factor at T_0 (no units)

2.18 Peak power rating of a photovoltaic solar cell

The rated or peak power of a photovoltaic solar cell, module or array is defined as its power output at the rated voltage under standard testing conditions (STC), the rated voltage is the nominal operating voltage at which the device is designed to produce near maximum power at STC. The rated power is normally expressed in terms of peak watts, peak kilowatts or peak megawatts (Wp, kWp or MWp). The performance of a photovoltaic device, be it a cell, a module, a sub-array or an array, is determined by exposing it at a known temperature to stable sunlight, natural or simulated, and tracing its current –voltage characteristics, while at the same time measuring the incident irradiance. If desired, the measured characteristic may then be transposed to Standard Testing Conditions or some other irradiance and /or temperature.

The performance of a crystalline silicon solar cell is very sensitive to the spectral irradiance distribution of the incident radiation. The same applies to all other types. With natural sunlight, spectral content varies with location, weather, time of the year and time of the day. With a solar simulator, it depends on the light source and the optical system and can be affected by ageing. If the irradiance is measured with an instrument that is not spectral selective, such as a pyranometer, spectral changes can affect outdoor measurements by as much as 15%. Moreover, the measurements cannot be related to a reference spectral irradiance distribution for rating purposes. This problem is overcome by measuring the irradiance with a reference device that has essentially the same relative spectral response as the test specimen and has been calibrated in terms of the short circuit current per unit of irradiance ($A.W^{-1}m^2$) which it would generate in radiation of the reference spectral distribution. Such a device automatically measures the irradiance in terms of the reference distribution, in so far as it affects the test specimen. Because of this, location, time and weather conditions are not so critical in outdoor measurements, neither is the quality of the simulator so critical indoors. Furthermore, since the reference device, unlike a radiometer, has the same time constant as the test specimen, some fluctuation in the irradiance can be accepted. If the measured performance is related in this way to a reference spectral

irradiance distribution and the spectral response of the test specimen is known, it is possible to compute with the reasonable accuracy the performance in radiation of a different spectral content [19].

CHAPTER-3

RESEARCH METHODOLOGY AND EXPERIMENTAL CONSIDERATIONS

3.1 Introduction

This chapter aims to provide methods employed in the design, construction, and mounting of a 0.45kWp PV array system as well as the collection of different types of data to achieve the desired results. The methodology includes literature review, field research in a region where PV array systems have been installed. The field research is intended mainly to determine the amount of solar radiation as well as the air temperature in the study area, measurements of the electrical power generated by PV array system; investigate PV array system performance, experience with the care and maintenance of PV array system, experience with failure and replacement of PV array systems, and monitoring protocols. Experimentation was carried out at the Vuwani science resource center of university of Venda in Limpopo province, South Africa of geographical coordinates: -23^{0}07`30.66``S, 30$^0$25`27.64``EAs part of the research project work plan, preliminary fieldwork was undertaken during 06 July 2009 - 15 July 2009 (see figure3.1) in order to evaluate the potential of solar electricity for the site.

Figure 3.1.Experimental site (preliminary field work)

3.2 Design

The installed photovoltaic array consists of six solar panels. Each PV solar panel has a rated electrical power of 75W at Standard Testing Conditions ($1000 W.m^{-2}, 25^{0}C$, Air Mass value of 1,5) and consists of 36 cells. Each individual panel has a rated short circuit current, open circuit voltage, maximum peak current and maximum peak voltage of 4.80A, 21.7V, 4.34A and 17.3V respectively. Panels were electrically connected to form two strings, each string consisting of three panels in series to produce high peak voltage and open circuit voltage of 51.9V and 65.1V respectively. These two strings were then electrically connected in parallel to maximize both the peak current and short circuit current. The overall short circuit current and peak current of the array are 8.68A and 9.6A respectively .The dimension of the entire array of two connected strings is $3.375 m^{2}$.

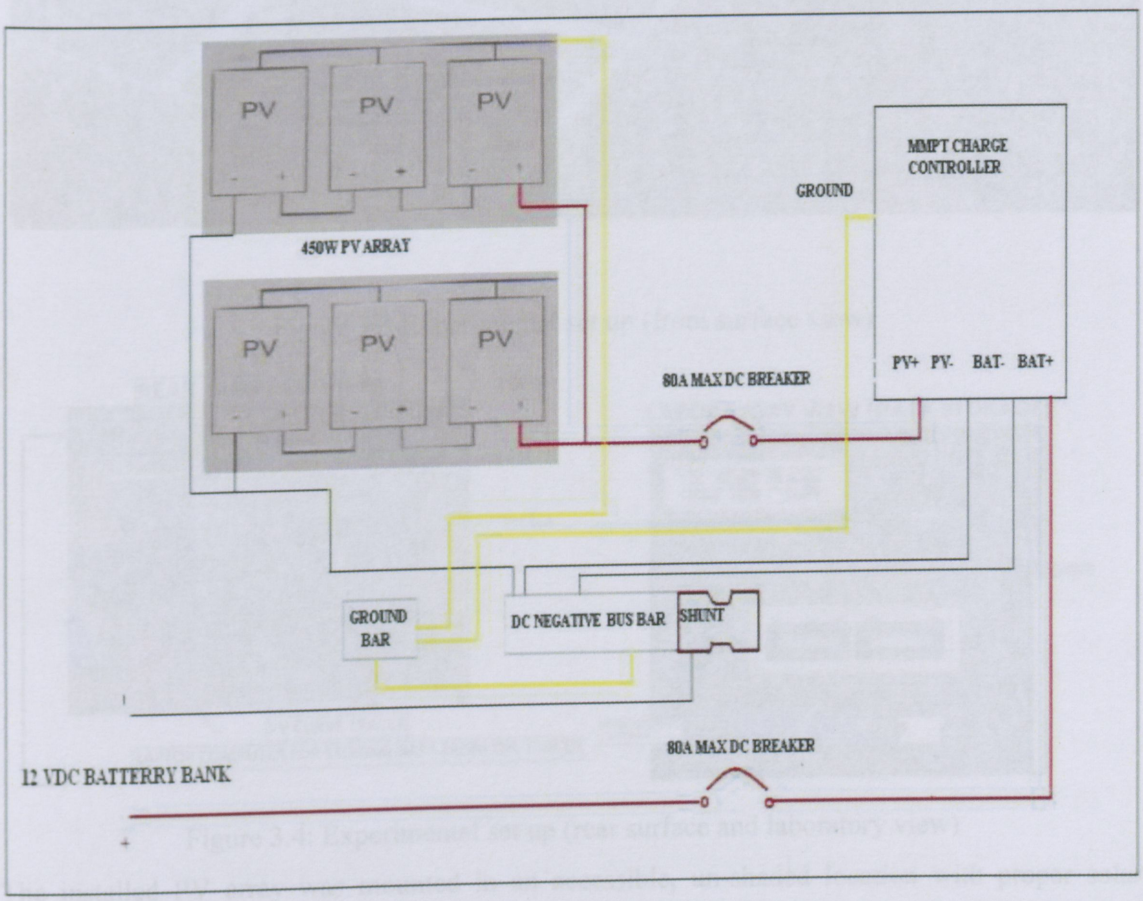

Figure 3.2 single charge controller wiring diagram with 450W PV array

3.3 Construction and mounting

This section describes how the PV array system was constructed and mounted. Two copper wires each with length of about11m and 23mm in diameter were used to connect the MPPT and the PV array. Individual panel specifications and overall system (PV array) specification are shown in appendix A.

Figure 3.3 Experimental set up (front surface view)

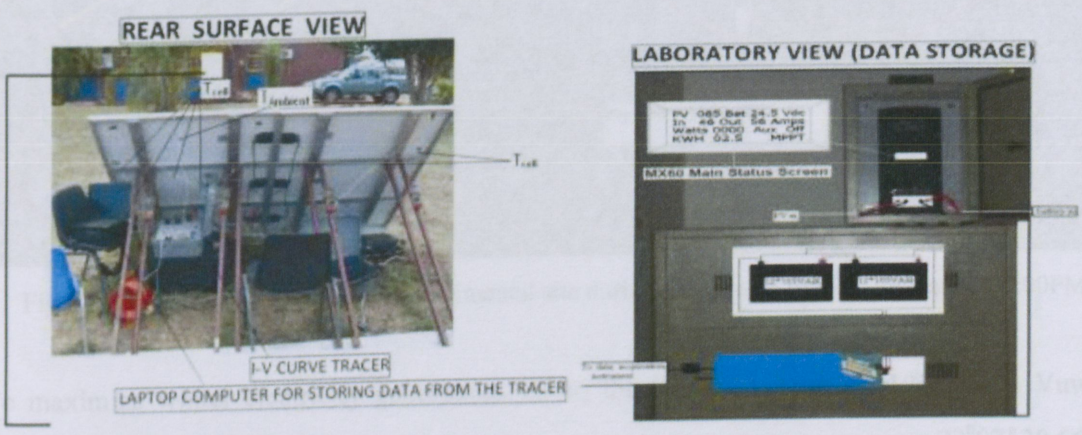

Figure 3.4: Experimental set up (rear surface and laboratory view)

The installed PV array was mounted in an accessible, un-shaded location with proper solar orientation and mounted on the ground and it is made of durable structure that can support the

array, and withstand wind, rain, hail, and other outdoor conditions. The PV array was mounted facing solar north, which differs from magnetic north. Since PV modules are extremely sensitive to shading, cells within a PV module and PV modules within an array were connected in series to give high peak current. For example, if one PV module in an array of six modules is completely shaded, it can reduce the output power of the entire array by 100%. In addition, given that the module will be acting as a resistor stopping the current flow, it will heat up to the point where it can become damaged. Therefore, when evaluating the location to mount a PV array, a shading analysis was performed to identify when and where shading will occur taking into consideration that during the winter months the sun is lower in the sky and tall objects, such as trees and buildings, cast longer shadows. See the figure below which illustrates the shading analysis.

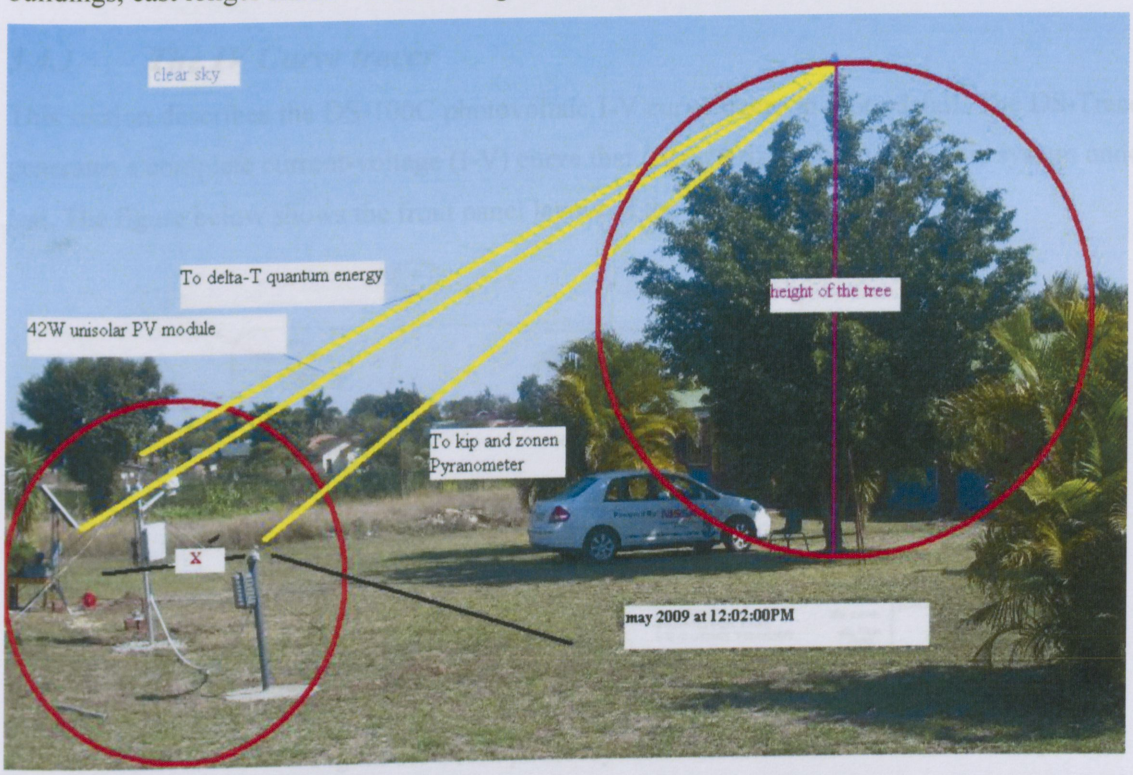

Figure 3.5 Shading analysis at the experimental site during the months of may 2009 at 12:02:00PM

To maximize winter electricity generation, 15° to the latitude was added[19]. At the Vuwani science resource center in Vuwani region as mentioned above, the latitude is $-23^{0}07"30.66"S$. The PV array was tilted at 38° (23° + 15° = 38°) up from the horizontal plane of the ground. To maximize electricity generation from the summer sunlight, 15° degrees from the latitude to find

the proper tilt angle was subtracted from the latitude [19]. At the Vuwani science resource center, to maximize summer sunlight, the PV array should be tilted at 8° (23° - 15° = 8°).

3.4 Data collection

Different types of data were collected using different measuring instruments. These instruments include I-V Curve tracer, delta-T weather station as well as the maximum power point tracking. Measured data include global solar radiation, short circuit current, open circuit voltage, peak voltage, peak current, and peak voltage and the cell temperature.

3.4.1 The IV Curve tracer

This section describes the DS-100C photovoltaic I-V curve tracer in more detail. The DS-Tracer generates a complete current-voltage (I-V) curve that characterizes the photovoltaic system under test. The figure below shows the front panel layout of the DS-100C [22].

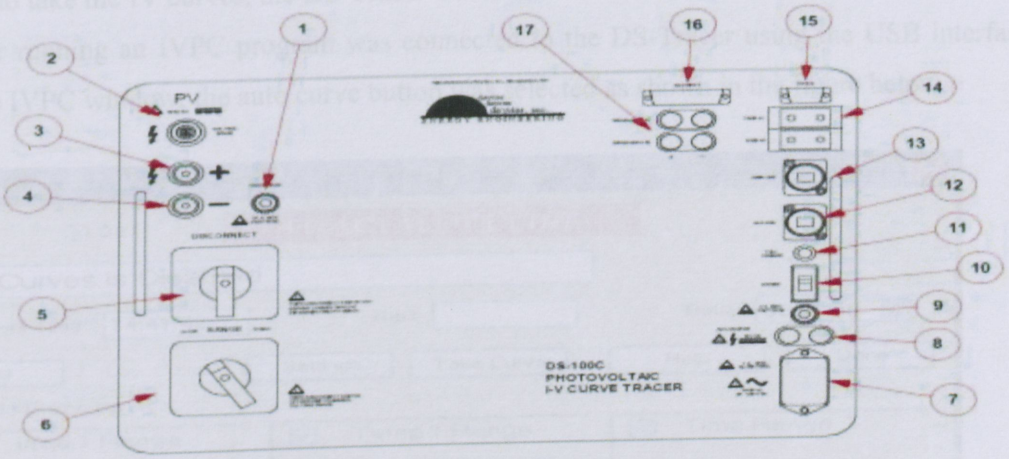

Figure 3.6 Front panel layout of the DS-100C

The DS-100C IV Tracer provides two interfaces; an RS-232 and USB port. The RS-232 interface uses a standard female 9 pin connector as shown front panel layout of the tracer. Only one of these ports was used at a time. The DS-Tracer was connected to the PV array with the test leads provided. Before connecting a PV module, care was taken to ensure that the DS-Tracer power switch is ON and the disconnect switch is in the OFF position. The test leads were attached to the PV module With the DS-Tracer disconnect switch still OFF. After

connecting the test leads, the PV system switch was then closed. The DS-Tracer DISCONNECT switch was turned to ON position. The DS-Tracer DISCONNECT switch was always at the last switch closed and the first switch opened. The figure below illustrates how the PV array system was connected to the tracer [22].

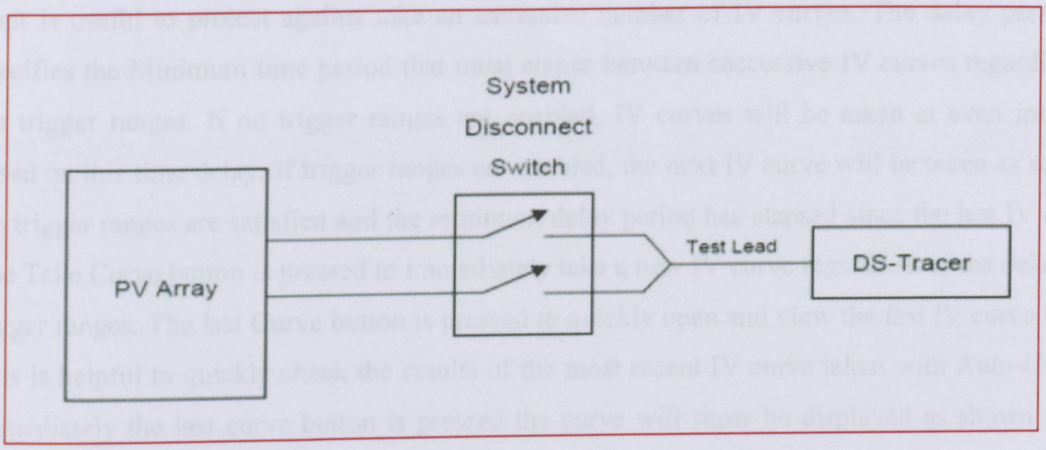

Figure 3.7 PV array system was connected to the tracer

In order to take the IV curves, the DS-Tracer was turned on and connected to the PV system. The computer running an IVPC program was connected to the DS-Tracer using the USB interface. From the IVPC window, the auto curve button was selected as shown in the figure below.

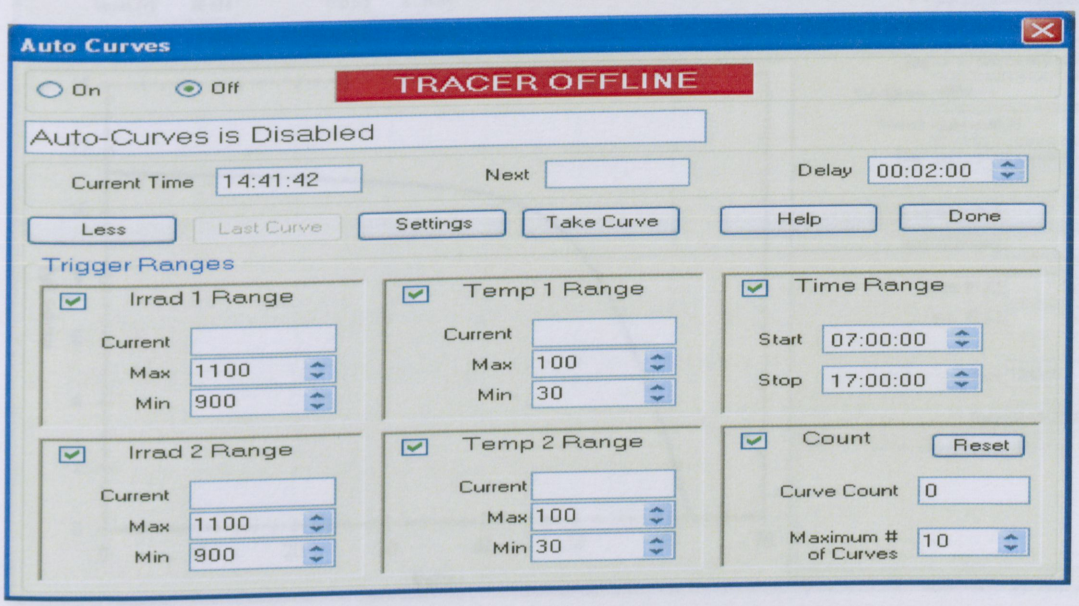

Figure3.8 The auto curve window

The Auto-Curves enable IVPC to automatically take IV curves at defined intervals and within preset conditions. By defining the conditional "Trigger Ranges" for taking a curve, IVPC and the IV tracer can be set to take curves under very specific conditions of time, irradiance, and temperature. Trigger includes irradiance, temperature, time and curve count limit. The curve limit is useful to protect against take an excessive number of IV curves. The delay parameter specifies the Minimum time period that must elapse between successive IV curves regardless of the trigger ranges. If no trigger ranges are enabled, IV curves will be taken at even intervals based on this time delay. If trigger ranges are enabled, the next IV curve will be taken as soon as the trigger ranges are satisfied and the minimum delay period has elapsed since the last IV curve. The Take Curve button is pressed to immediately take a new IV curve regardless of the delay and trigger ranges. The last Curve button is pressed to quickly open and view the last IV curve taken. This is helpful to quickly check the results of the most recent IV curve taken with Auto-Curves. Immediately the last curve button is pressed the curve will show be displayed as shown in the figure below.

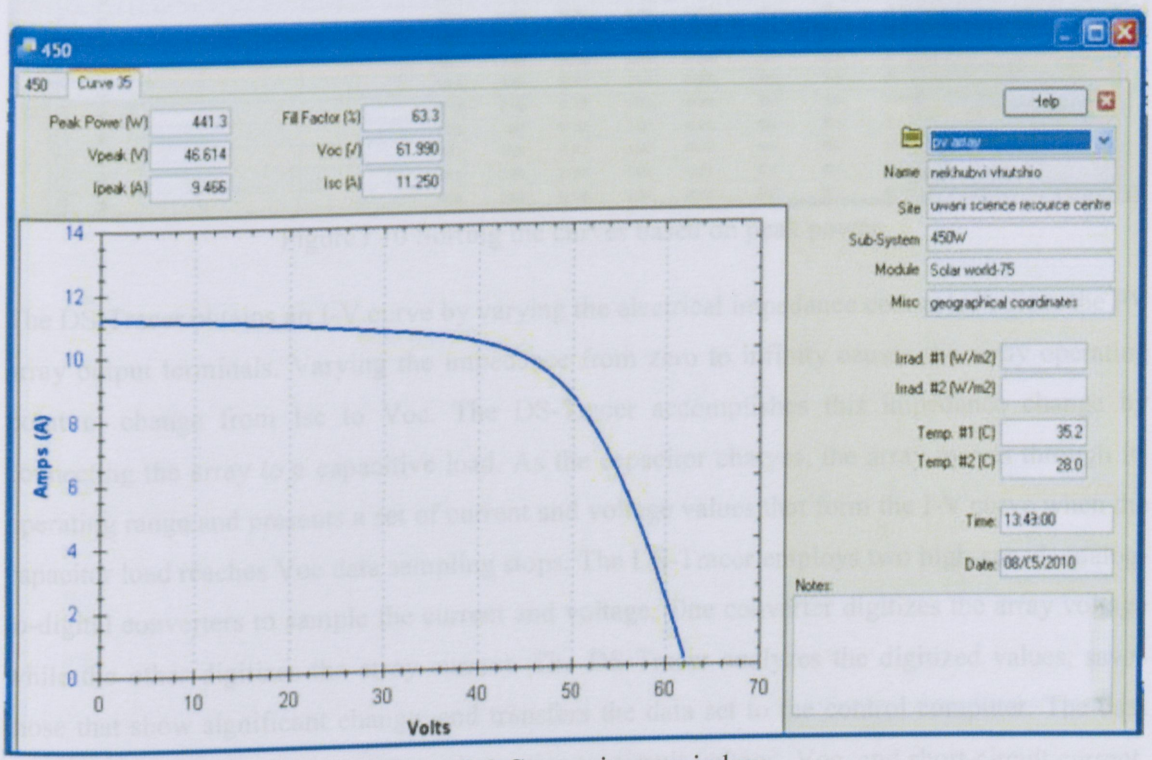

Figure3.9 Curve viewer window

The curve list view displays all IV curves in a worksheet and is the primary data view. A worksheet always has one and only one Curve List view. The Curve List displays IV curve data as rows within a spreadsheet. The spreadsheet has multiple columns presenting key information about the IV curve such as Name, Peak Power, Voc, etc. the IV Curves can sorted by clicking on the column header. For example to sort the curves based on peak power, the peak power column header as shown in the figure below is clicked [22].

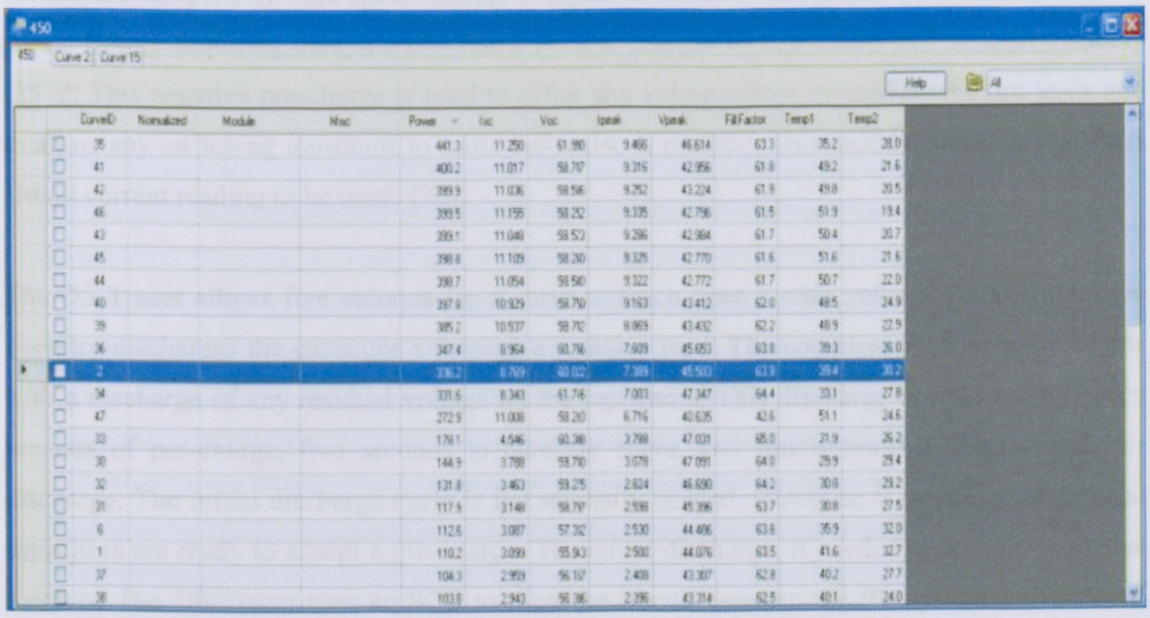

Figure3.10 Sorting the curves based on peak power

The DS-Tracer obtains an I-V curve by varying the electrical impedance connected across the PV array output terminals. Varying the impedance from zero to infinity causes the array operating point to change from Isc to Voc. The DS-Tracer accomplishes this impedance change by connecting the array to a capacitive load. As the capacitor charges, the array moves through its operating range and presents a set of current and voltage values that form the I-V curve when the capacitor load reaches Voc data sampling stops. The DS-Tracer employs two high-speed, analog-to-digital converters to sample the current and voltage. One converter digitizes the array voltage while the other digitizes the array current. The DS-Tracer analyzes the digitized values, saves those that show significant change, and transfers the data set to the control computer. The data sets include the I-V curve data plus values of open-circuit voltage, Voc, and short-circuit current, Isc. Peak-power, voltage at peak-power Vpk, current at peak-power Ipk, and fill factor are

calculated and displayed with the curve. Irradiance and temperature data, and array identification may be added to each data set. The irradiance and temperature data are either entered by the operator using IVPC or sampled by the DS-100C.The DS-Tracer sweeps an I-V curve by switching the PV system to a bank of capacitors. As these capacitors charge, the PV system voltage increases until open circuit voltage is reached. While the voltage is increasing, and the current to the capacitors is decreasing from its maximum, short-circuit value, the voltage and current are sampled by high-speed analog-to-digital converters. These data points define the I-V curve. Before acquiring data, the DS-Tracer reverse charges its capacitive load to approximately -25 V. This negative pre-charge is used to offset any voltage drops created by the test leads and to allow any switching transients to settle before Isc is reached. This method allows a true short circuit current reading to be made [22].

The DS-Tracer allows five seconds for a curve to reach open circuit voltage. At this point the circuitry discharges the capacitor s through a resistive load. The complete cycle actually begins with a discharge of any residual voltage on the capacitors. This discharge is followed by seven seconds of pre-charge, five seconds to take the curve, and finally another five seconds for discharge. The initial discharge cycle is not normally needed. However, it ensures that the load capacitors are ready to accept a pre-charge. The initial discharge, if needed, may take up to five seconds. The DS-Tracer uses an SCR to close the circuit between the PV system and the load capacitors. SCRs are susceptible to false triggering (turn on) if the voltage across them is increased too rapidly. The DS-Tracer DISCONNECT switch uses two 1MΩ resistors (one each for the positive and negative leads) across the disconnect switch contacts. These resistors allow the SCR to check the PV system voltage before the DISCONNECT switch is closed; thereby preventing the SCR from false triggering when the disconnect switch is closed. Under normal operating conditions, this switch should always be the last switch closed and the first switch opened when making PV system connections.

Some PV systems are sensitive to how quickly an I-V curve is taken. The speed of a curve is most easily expressed in volts per second by taking the PV short circuit current in Amps (Isc) and dividing it by the DS-Tracer load capacitance in Farads. Often the PV module manufacturer can provide information concerning how quickly an I-V curve can be swept on their modules.

Standard Type-T thermocouple connectors were available and were connected to the tracer and the PV array in order to accurately acquire temperature data, only matching thermocouple types were used. The thermocouple inputs were electrically isolated from the PV system, but not isolated from other analog circuits or the computer connections. Therefore, it is necessary that the thermocouple be electrically insulated when bonded to a surface (as in figure 3.4).

3.4.2 *The delta-T weather station*

Figure 3.11 Delta-T weather station used to record global solar radiation and air temperature

The determination of solar radiation enhanced the knowledge of the actual amount of solar energy resources available in the study area. In this research project, the amount of solar energy falling on the experimental site was determined. The most reliable way of determining solar radiation falling on the experimental site was by direct measurement. The following instrument was of major use when measuring solar radiation in the study area; Delta -T weather station. The global solar radiation intensity data was collected for the period of five months from February 2010 to June 2010 on hourly bases.

This section describes how to use logger, and how to adapt it, or create a new program for the weather station. The Delta-T Weather Station uses the DL2e Logger as its data recording unit. The DL2e logger is a general-purpose programmable data logger. The DL2e logger unit contains

all the hardware required for capturing and storing data from a wide variety of different types of sensor, under most environmental conditions. It runs an internal logging program that is set up by the user, and tells the logger how and when to acquire data. The logger's front panel keypad and display gives control over the essential features which are needed for field operation away from a computer, such as starting and stopping the logger, displaying current readings, providing status reports, and outputting logged data to a local printer or intermediate collection device. The Windows software Ls2Win also provides control over all the features available from the front panel keypad and it is also used to program the logger. This involves choosing the number of channels to be logged, the types of sensor and appropriate data conversions, the rate at which each channel is to be logged, and action to be taken on out of limits conditions. It also provides a range of other features that are not available from the keypad, such as timed start, triggering on events, collecting and manipulating logged data.

User can assemble the weather station and connect sensors on site, and perform sensor checks under actual operating conditions. If one does so, one will need a battery-powered portable PC to view sensor application notes (including wiring information) and for sensor checks or you will have to rely on the logger's front panel keypad and display. Alternatively, with a little ingenuity, it is possible to do all the preparation for logging in the comfort of the office including electrical connections, sensor checks and setting the logger to start logging and defer onsite installation until the system is ready to actually record data [23].

If user wants to select the time when logging will start, user must enable Defer first TIMED data until and select the date and time that he requires as shown in the figure below.

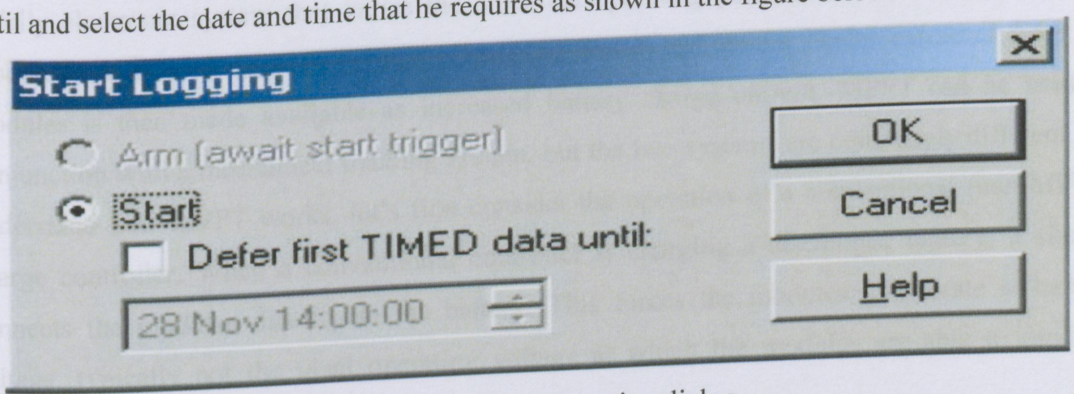

Figure 3.14 Start Logging dialog

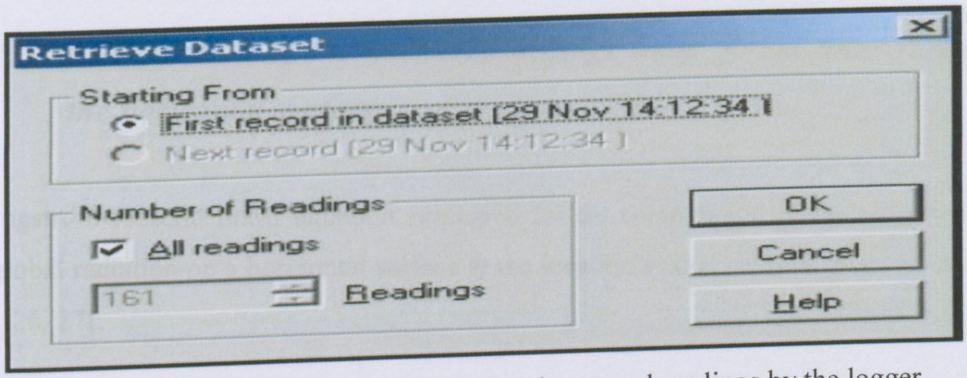

Figure 3.15 Retrieve dataset dialog showing stored readings by the logger

To finish this process the user must click the OK button to return to the Logger panel, and observe that the program status changes to LOGGING. User must leave his logger logging for a few minutes, hour, and days to create some data. On the Dataset panel click Refresh to update the display showing how many readings are stored as shown in the figure below

3.4.3 The maximum power point tracking charge controller(MPPT)

The Flex max 60 maximum power point tracking charge controller features continuous maximum power point tracking which seeks out the maximum power available from a PV array. The charge controller continuously tracks the array's maximum operating power. Last 128 days of operational data are logged for review. Maximum Power Point Tracking, frequently referred to as MPPT, is an electronic system that operates the PV modules in a manner that allows the modules to produce all the power they are capable of [24]. MPPT is not a mechanical tracking system that physically moves the modules to make them point more directly at the sun. MPPT is a fully electronic system that varies the electrical operating point of the modules so that the modules are able to deliver maximum available power. Additional power extracted from the modules is then made available as increased battery charge current. MPPT can be used in conjunction with a mechanical tracking system, but the two systems are completely different. To understand how MPPT works, let's first consider the operation of a conventional (non-MPPT) charge controller. When a conventional controller is charging a discharged battery, it simply connects the modules directly to the battery. This forces the modules to operate at battery voltage, typically not the ideal operating voltage at which the modules are able to produce maximum power [25].

3.4.4 *Computation of the estimated average daily global solar radiation on the horizontal surface.*

The Angström-Prescott linear equation employed for the computation of the estimated average daily global radiation on a horizontal surface at the location in this study is given by the relation below [26, 27]:

$$\frac{\overline{H}}{H_0} = a + b\frac{S_a}{S_p} \tag{3.1}$$

where S_a represents the daily average of duration of actual sunshine hours, $S_p$represents the daily average duration of possible sunshine hours, $\overline{H}$representsthe estimated daily average of the global radiation on a horizontal surface, $\overline{H}_o$represents the average of the daily extraterrestrial radiation on a horizontal surface on clear days at the same location, and a and b are the revised empirical constants/regression coefficients. As one observes the above equation, a number of variables such as $a,b$and $S_a$need to be known while S_p and $\overline{H}_o$are computed. Micro office excel is employed to compute the daily average global solar radiation of the study area whereby equation 1 is now written as:

$$\overline{H} = \left(a + b\frac{\overline{S_a}}{S_p}\right)\overline{H_o} \tag{3.2}$$

3.4.4.1 *The daily average extraterrestrial global solar radiation ($\overline{H}_o$)*

The daily extraterrestrial radiation on a horizontal surface, $\overline{H}_o$, is calculated as a function of the solar constant (I_{sc}), the latitude of the location on study (ϕ), the eccentricity correction factor of the Earth's orbit (E_o), the solar declination $(\delta)$and the mean sunrise hour angle (ω_s) using Equation 2 [28, 29].

$$\overline{H_0} = \frac{24}{\pi} I_{sc} E_o \left(\cos\delta \cdot \cos\phi \cdot \sin\omega_s + \frac{\pi w_s}{180} \sin\phi \cdot \sin\omega_s \right) \quad (3.3)$$

where $E_o = 1 + 0.033 \cos \frac{360n}{365}$

where I_{sc} is the solar constant which is defined as the amount of energy received at the top of the Earth's atmosphere measured at an average distance between the Earth and the Sun on a surface oriented perpendicular to the Sun. The generally accepted solar constant has been approximated as 1367 Wm^{-2} by the World Meteorological Organization (WMO),

n = the day of the year, running from day 1 to day 365 where day 1 is equivalent to the 1st January while day 365 is the 31st December of each year.

δ = solar declination angle, can be expressed as follows [30, 31]:

$$\delta = 23.45^0 \sin\left[\frac{360}{365}(284 + n)\right], \quad (3.4)$$

ϕ is the latitude of the location of the study its value was given in section 3.1 of this chapter and ω_s is the mean sunrise hour angle, in degrees and is expressed as [32]:

$$\cos w_s = -\tan\phi \cdot \tan\delta \quad (3.5)$$

Sunset hour angle depends on the solar declination angle and latitude of the geographical study area.

3.4.4.2 *Actual sunshine hours (S_a)*

In almost all the countries of the world, actual sunshine hours are measured at meteorological stations using Campbell Stokes sunshine recorder. In this study, the daily actual sunshine data measured in hours used, were obtained from the South African Weather Services (SAWS) for Thohoyandou. This station was selected to be used because its geographical properties are similar to the location in study such as the distance between them is less than 50 km, falling in the same region, same weather forecast, etc.

3.4.4.3 *Possible sunshine hours (S_p)*

The daily possible sunshine hours depend on the location in study and day of the year. This can be computed using the relation given below:

$$S_p = \frac{2\omega_s}{15}\cos^{-1}(-\tan\phi \cdot \tan\delta) \tag{3.6}$$

In the northern and southern hemispheres, the shortest day lengths are observed during winter season irrespective of the latitude.

3.5 Brief summary of measuring instruments

The delta-t data logger was used to measure solar radiation and the air temperature in the study area. Both the global solar radiation intensity and temperature data were collected for the period of five months from February 2010 to June 2010 on an hourly base from 07:H00 to 17H00.The maximum power point charge controller was used continuously to tracks the array's maximum operating power and stored data for collection. The controller started to record data from sunrise to sunset. The IV tracer was used to take curves under very specific conditions of time, irradiance, and temperature. Electrical parameters like peak voltage, peak current, short circuit current, open circuit voltage and the fill factor were recorded for peak power analyses purposes. Due to the failure of the delta-T data logger, the Angström-Prescott linear equation was employed for the computation of the estimated average daily global radiation on a horizontal surface at the location in this study. Both measured and estimated data were then used to analyze the peak power of an installed photovoltaic array in chapter 4.

CHAPTER-4

RESULTS, DISCUSSION AND CONCLUSIONS

4.1 RESULTS

4.1.1 Data analysis and graphical representation

It is often convenient to represent experimental data in graphical form, not only for reporting, but also to obtain information. The experimental results obtained from the present work were reported in this chapter. The experiment was conducted for normal mode as well as the disturbed mode i.e. for cloudy as well as clear day conditions. The measured data include the global solar radiation intensity, daily peak power, ambient temperature, PV array temperature, open-circuit voltage, maximum power point voltage; short-circuit current and maximum power point current. Due to the failure of the measuring instrument, the global solar radiation values were estimated from the sun hour duration data sourced from the South African weather station. Both the measured and estimated data were analyzed and treated in order to evaluate the performances of the PV array system, peak power analysis to be specific.

To avoid the problem of negative deviations and absolute values, it is statistically convenient to use the square of the deviation. Standard deviation is a widely used measurement of variability or diversity used in statistics and probability theory. It shows how much variation there is from the average or mean. The standard deviation is simply the root-mean-square because we take the average of the squares of the deviations and then the square root. A low standard deviation indicates that the data points tend to be very close to the mean; whereas high standard deviation indicates that the data are spread out over a large range of values. In the present work the results were reported based on standard deviation in order to describe the precision of the mean of the set of measurements especially when comparing the measured and rated peak power value of the solar panel.

4.1.1.1 *Measured global solar radiation data by the Delta-T data logger*

Below in table 4.1 is the data of the measured global solar radiation measured by the Delta-T data logger using the CM6B kipp and Zonen pyranometer. Measurements were made for the period of five months. As indicated in chapter 3, the data logger failed to respond from July to December 2010 and so it was decided to compute the estimated data. As depicted from the graph in figure 4.1 one can observe that for the month of February 2010 there is no data for day 1 and day 17 due to instrument failure.

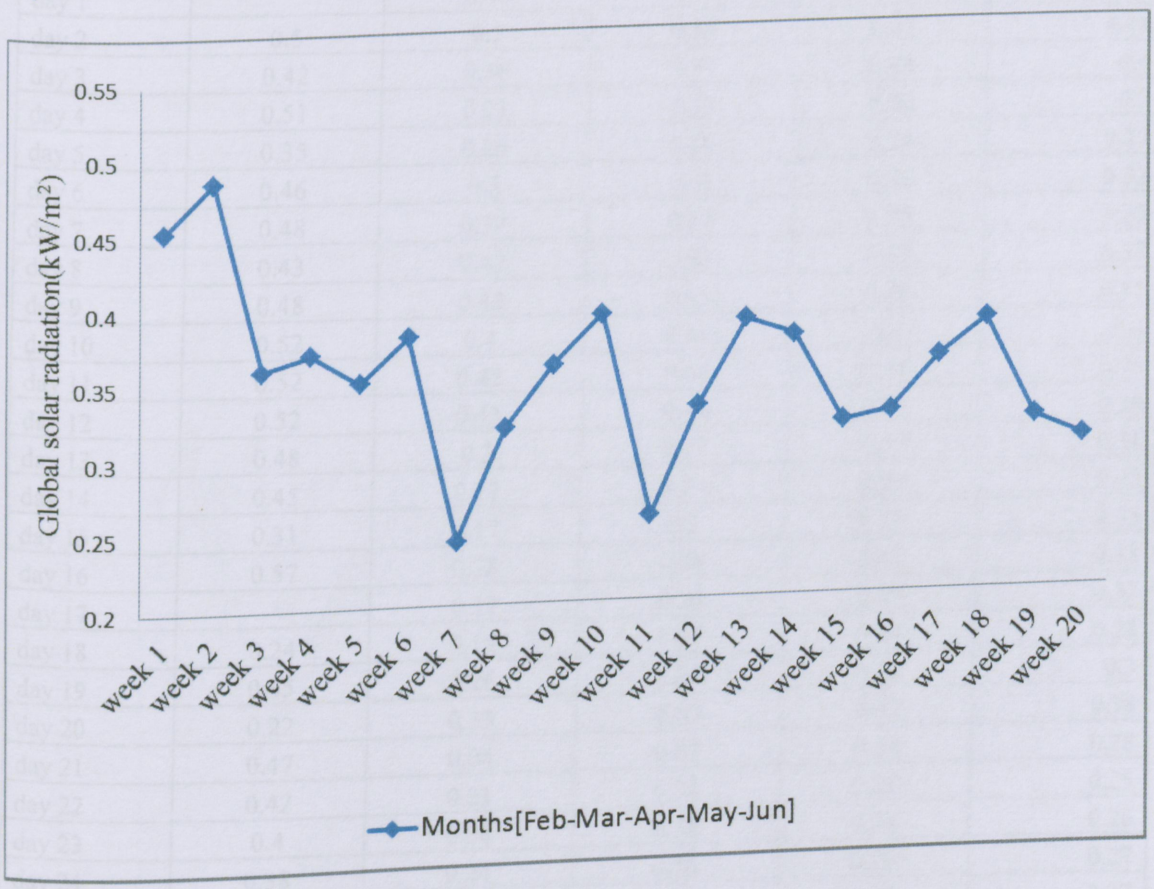

Figure 4.1 observed weekly global solar radiation for the months of the year 2010

For the month of February 2010 the maximum global solar radiation value was found to be 0.57KW/m^2. The pattern observed in table 4.1was totally different to the pattern of the estimated values since for the measured data, the decrease was not sequential but randomly. The pattern observed in table 4.1 also applied to the months of March, April, May and June. The minimum

value for the month of February was found to be 0.18KW/m^2. For the month of March the logger registered the maximum value of the global solar radiation of 0.5KW/m^2 and the minimum of 0.04KW/m^2.

Table 4.1 Measured global solar radiation by the delta-T data logger in (kW/m^2)

Days	February	March	April	May	June
day 1		0.45	0.45	0.45	0.39
day 2	0.5	0.5	0.52	0.52	0.44
day 3	0.42	0.36	0.37	0.46	0.4
day 4	0.51	0.21	0.23	0.26	0.3
day 5	0.35	0.26	0.26	0.29	0.29
day 6	0.46	0.3	0.31	0.33	0.33
day 7	0.48	0.37	0.37	0.39	0.35
day 8	0.43	0.42	0.43	0.37	0.37
day 9	0.48	0.42	0.43	0.46	0.41
day 10	0.52	0.4	0.41	0.4	0.4
day 11	0.52	0.42	0.44	0.38	0.39
day 12	0.52	0.43	0.44	0.37	0.39
day 13	0.48	0.3	0.32	0.37	0.38
day 14	0.45	0.27	0.27	0.27	0.33
day 15	0.31	0.17	0.2	0.23	0.32
day 16	0.57	0.38	0.38	0.41	0.33
day 17		0.37	0.38	0.37	0.32
day 18	0.24	0.15	0.17	0.24	0.28
day 19	0.35	0.26	0.26	0.26	0.3
day 20	0.22	0.33	0.33	0.42	0.38
day 21	0.47	0.04	0.07	0.28	0.28
day 22	0.42	0.21	0.24	0.25	0.25
day 23	0.4	0.38	0.38	0.34	0.26
day 24	0.38	0.24	0.26	0.27	0.27
day 25	0.39	0.36	0.36	0.33	0.27
day 26	0.39	0.36	0.37	0.38	0.38
day 27	0.18	0.33	0.34	0.37	0.37
day 28	0.43	0.34	0.35	0.31	0.31
day 29		0.13	0.18	0.25	0.25
day 30		0.39	0.4	0.45	0.45
day 31				0.42	

For the month of April the logger registered the maximum global solar radiation value of 0.52KW/m^2 and the minimum value of 0.07KW/m^2.For the month of May the logger registered the maximum global solar radiation of 0.52KW/m^2 and the minimum of 0.25KW/m^2. For the month of June the logger registered the maximum global solar radiation value of 0.45KW/m^2 and the minimum value of 0.25KW/m^2.

Looking at the graph of monthly average in figure 4.2 below one can observe that the logger registered the maximum value of the monthly average value of global solar radiation of 0.418KW/m^2 during the month of February 2010 and the minimum value of 0.318KW/m^2 during the month of March 2010. According to the theory the minimum was expected to be found during the month of June; however opposite is the case .The minimum value obtained during the month of March resulted from the cloudy day condition.

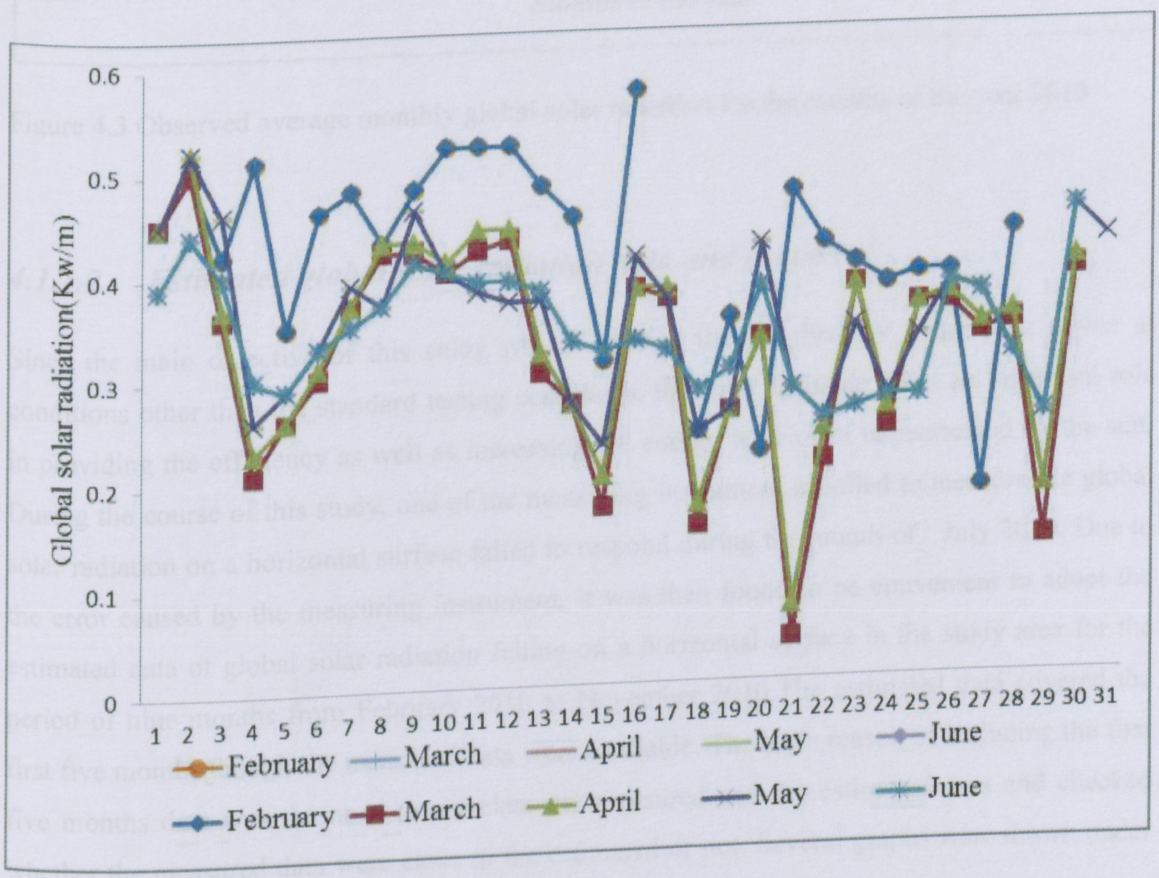

Figure 4.2 Observed monthly global solar radiation for the months of the year 2010

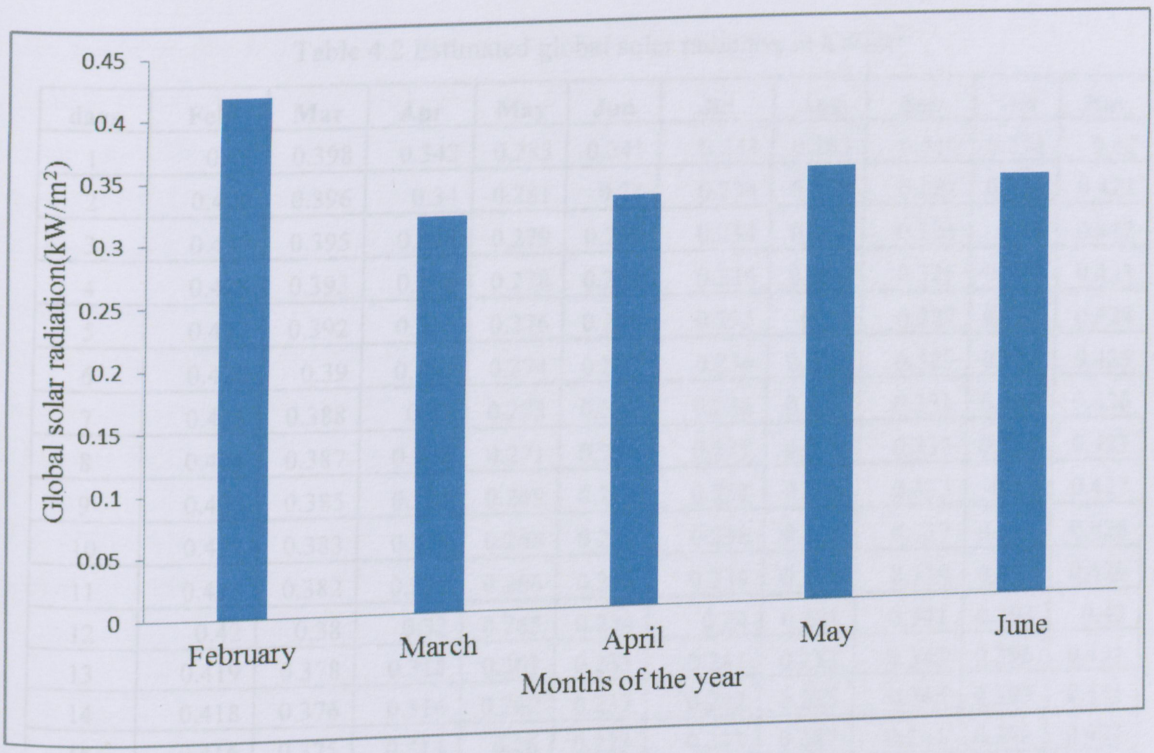

Figure 4.3 Observed average monthly global solar radiation for the months of the year 2010

4.1.1.2 Estimated global solar radiation data and graphs

Since the main objective of this study was to analyse the installed PV array peak power at conditions other than the standard testing conditions, the solar radiation plays an important role in providing the efficiency as well as increasing the energy which can be harnessed by the sun. During the course of this study, one of the measuring instrument installed to measure the global solar radiation on a horizontal surface failed to respond during the month of July 2010. Due to the error caused by the measuring instrument, it was then found to be convenient to adopt the estimated data of global solar radiation falling on a horizontal surface in the study area for the period of nine months from February 2010 to November 2010.The estimated data covered the first five months though the measured data were available. The main reason of including the first five months data was the need to correlate the measured and the estimated data and checked whether the measured data were close to the estimated or not. Several graphs were drawn under estimated global solar data recorded in the table 4.2.

Table 4.2 Estimated global solar radiation in kW/m^2

days	Feb	Mar	Apr	May	Jun	Jul	Aug	Sep	Oct	Nov
1	0.43	0.398	0.342	0.283	0.241	0.233	0.263	0.319	0.376	0.42
2	0.429	0.396	0.34	0.281	0.24	0.234	0.265	0.321	0.378	0.421
3	0.429	0.395	0.338	0.279	0.239	0.234	0.266	0.323	0.38	0.422
4	0.428	0.393	0.336	0.278	0.238	0.235	0.268	0.325	0.382	0.423
5	0.427	0.392	0.334	0.276	0.238	0.235	0.27	0.327	0.383	0.424
6	0.426	0.39	0.332	0.274	0.237	0.236	0.271	0.329	0.385	0.425
7	0.425	0.388	0.33	0.273	0.236	0.236	0.273	0.331	0.386	0.426
8	0.424	0.387	0.328	0.271	0.236	0.237	0.274	0.333	0.388	0.427
9	0.423	0.385	0.326	0.269	0.235	0.238	0.276	0.335	0.39	0.427
10	0.422	0.383	0.324	0.268	0.235	0.238	0.278	0.337	0.391	0.428
11	0.421	0.382	0.322	0.266	0.234	0.239	0.279	0.339	0.393	0.429
12	0.42	0.38	0.32	0.265	0.234	0.24	0.281	0.341	0.394	0.43
13	0.419	0.378	0.318	0.263	0.233	0.241	0.283	0.343	0.396	0.431
14	0.418	0.376	0.316	0.262	0.233	0.242	0.285	0.345	0.397	0.431
15	0.416	0.375	0.314	0.26	0.233	0.243	0.287	0.347	0.399	0.432
16	0.415	0.373	0.312	0.259	0.232	0.244	0.288	0.349	0.4	0.433
17	0.414	0.371	0.31	0.257	0.232	0.245	0.29	0.351	0.402	0.434
18	0.413	0.369	0.308	0.256	0.232	0.246	0.292	0.353	0.403	0.434
19	0.412	0.367	0.306	0.255	0.232	0.247	0.294	0.355	0.404	0.435
20	0.41	0.365	0.304	0.253	0.232	0.248	0.296	0.356	0.406	0.436
21	0.409	0.363	0.302	0.252	0.232	0.249	0.298	0.358	0.407	0.436
22	0.408	0.362	0.3	0.251	0.232	0.25	0.3	0.36	0.408	0.437
23	0.406	0.36	0.298	0.25	0.232	0.251	0.302	0.362	0.41	0.437
24	0.405	0.358	0.296	0.249	0.232	0.252	0.303	0.364	0.411	0.438
25	0.404	0.356	0.294	0.247	0.232	0.254	0.305	0.366	0.412	0.438
26	0.402	0.354	0.292	0.246	0.232	0.255	0.307	0.368	0.413	0.439
27	0.401	0.352	0.29	0.245	0.232	0.256	0.309	0.369	0.414	0.439
28	0.399	0.35	0.288	0.244	0.232	0.258	0.311	0.371	0.416	0.44
29	0	0.348	0.287	0.243	0.233	0.259	0.313	0.373	0.417	0.44
30	0	0.346	0.285	0.242	0.233	0.26	0.315	0.375	0.418	0.441
31	0	0.344	0	0.241	0	0.262	0.317	0	0.419	0
aver	0.416	0.372	0.313	0.26	0.234	0.245	0.289	0.347	0.399	0.432

The drawn graphs were for the weekly (figure 4.4 to 4.6), monthly (figure 4.7) and average monthly (figure 4.8) graphs. Looking at the graphs of weekly global solar radiation below, the maximum value of the global solar radiation falling on the horizontal plane was estimated to be 0.441kW/m^2.The minimum value of the global solar radiation was estimated to be 0.232kW/m^2.For the month of February, one could notice that there was a decrease in global solar radiation value from the first day until the last day of the month. The same applied also for the months, March, April, May and June 2010. For the month of July, one could notice that there was an increase in global solar radiation value from the first day until the last day of the month. The same applied also for the month of August, September, October and November 2010.

The decrease in the global solar radiation values was also depicted in the monthly average of the global solar radiation graphs in figure 4.4where as for the months February, March, April, May and June the values were dropping to zero.

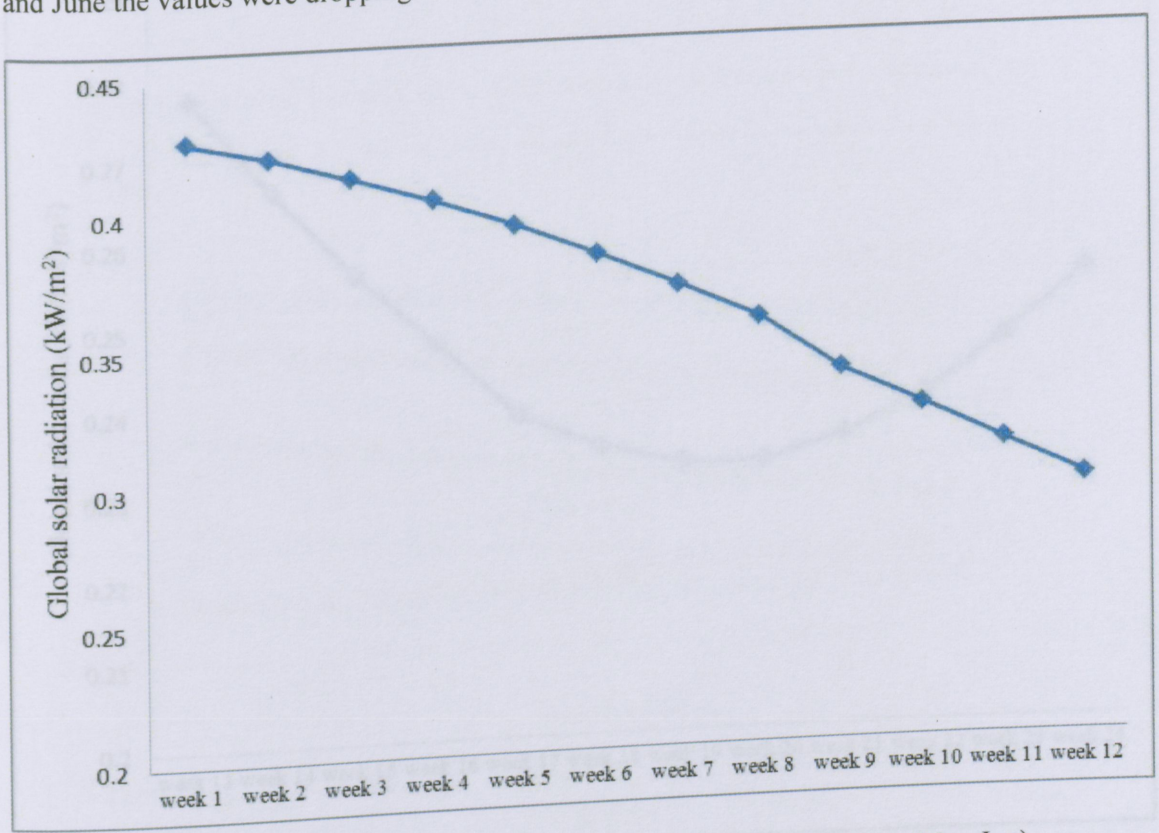

Figure 4.4 Estimated weekly global solar radiation for the months (Apr-May-Jun)

The increase in global solar radiation was shown as well during the months of July, August, September, October and November 2010. If one could look at the monthly average graph in figure 4.8, one could notice that the highest value of the average monthly global solar radiation was found during the month of November 2010 followed by the value obtained during the month of June which was the only month with the smallest value of the global solar radiation according to the graph. The present work is geared towards finding the meaningful relationship between the global solar radiation and the PV array peak power. The peak power analysis is explained in detail in section 4.1.1.4

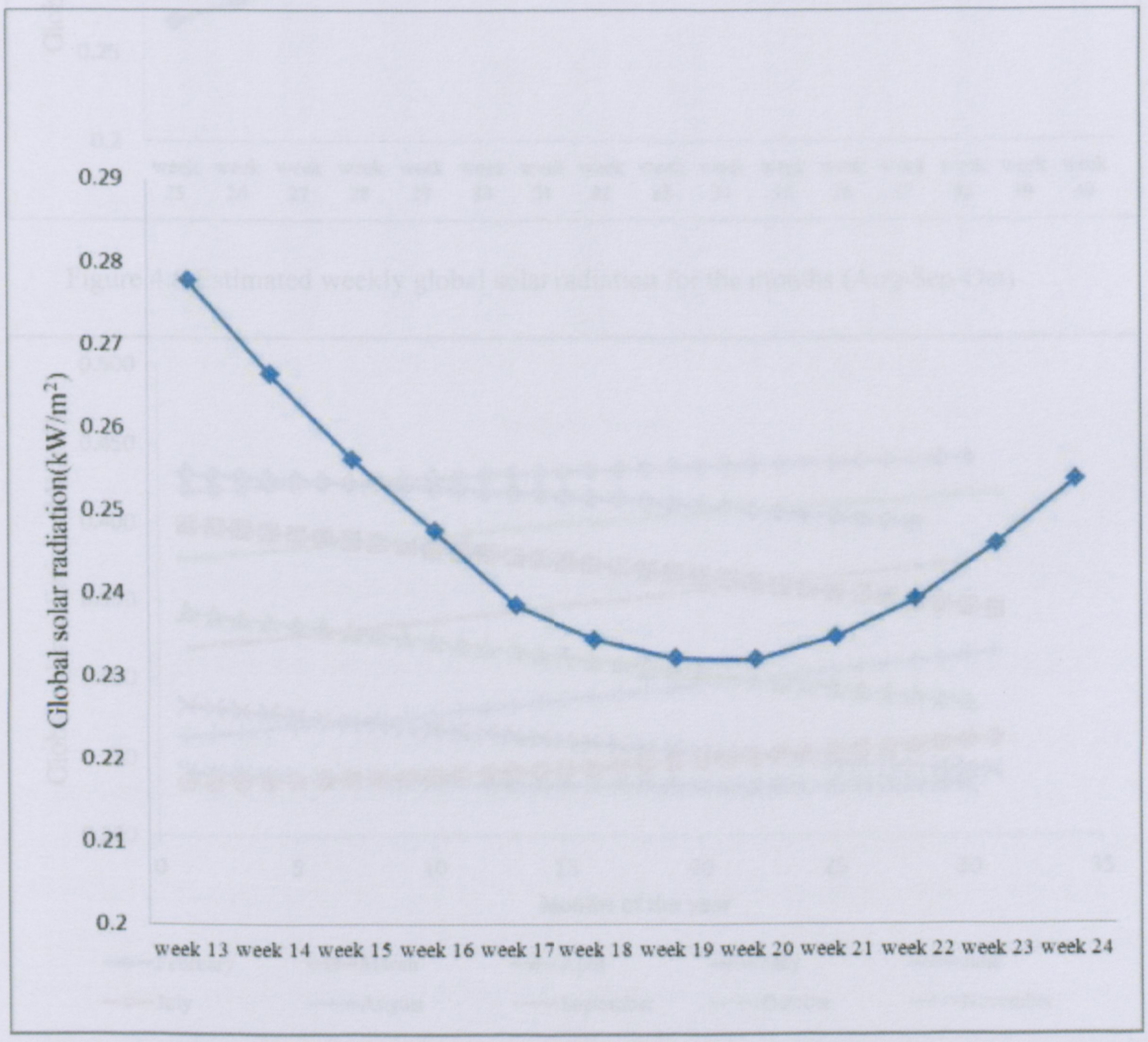

Figure 4.5 Estimated weekly global solar radiation for the months (May-Jun-Jul)

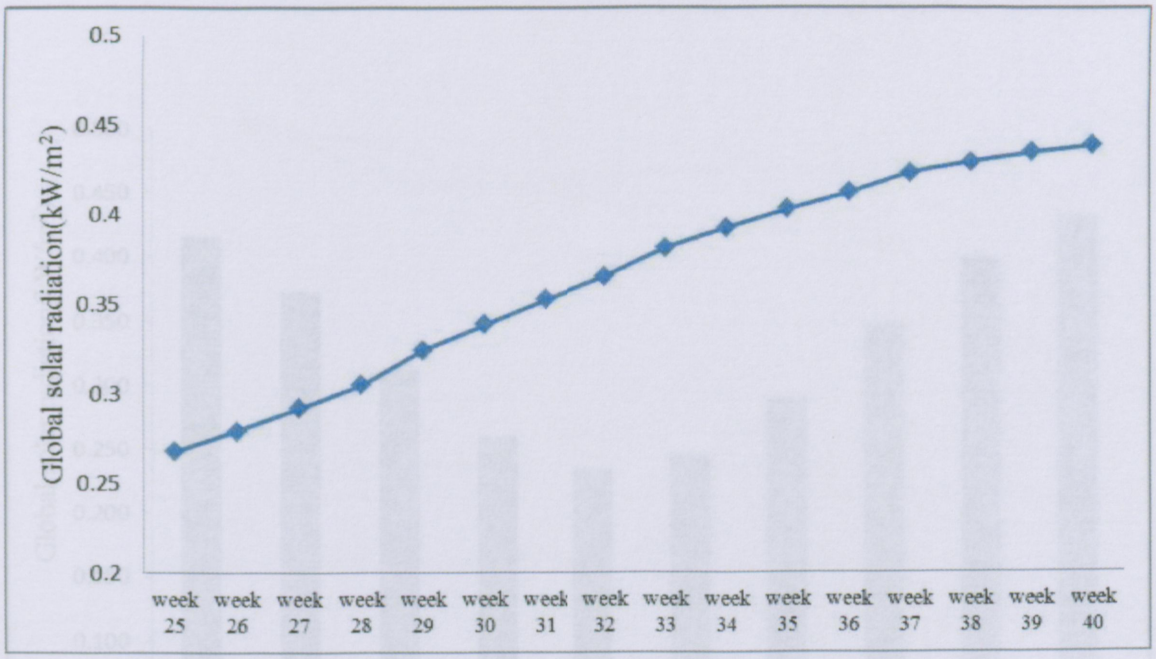

Figure 4.6 Estimated weekly global solar radiation for the months (Aug-Sep-Oct)

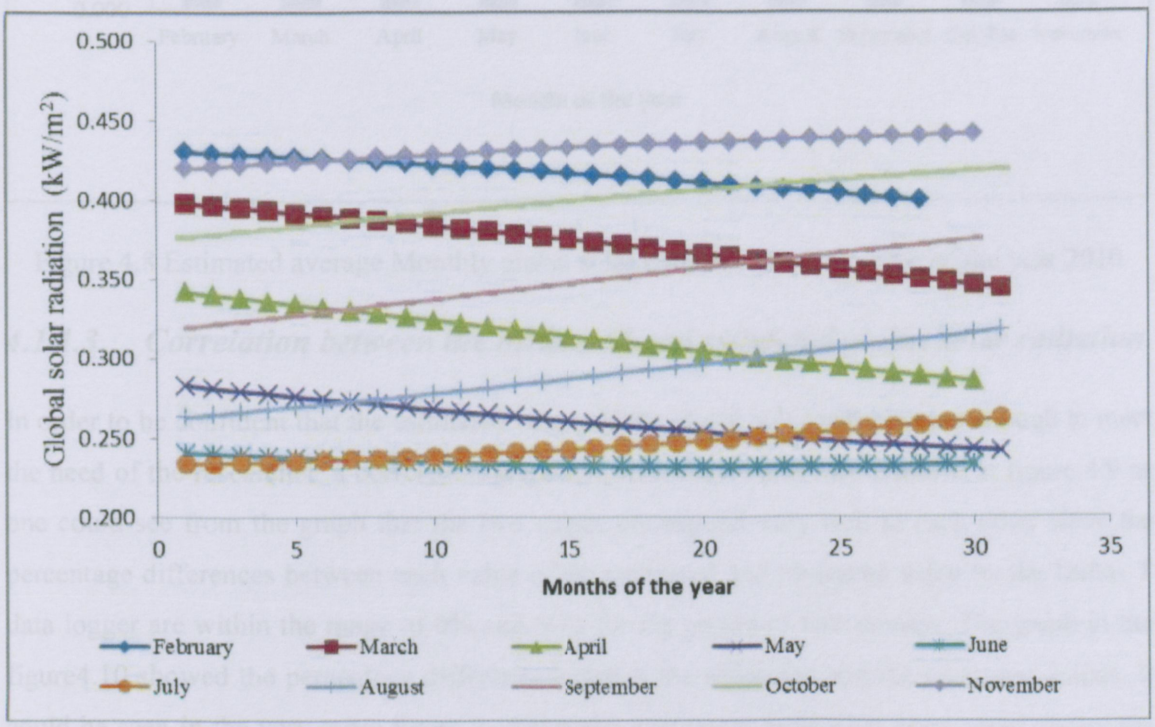

Figure 4.7 Estimated monthly global solar radiation for the months of the year 2010

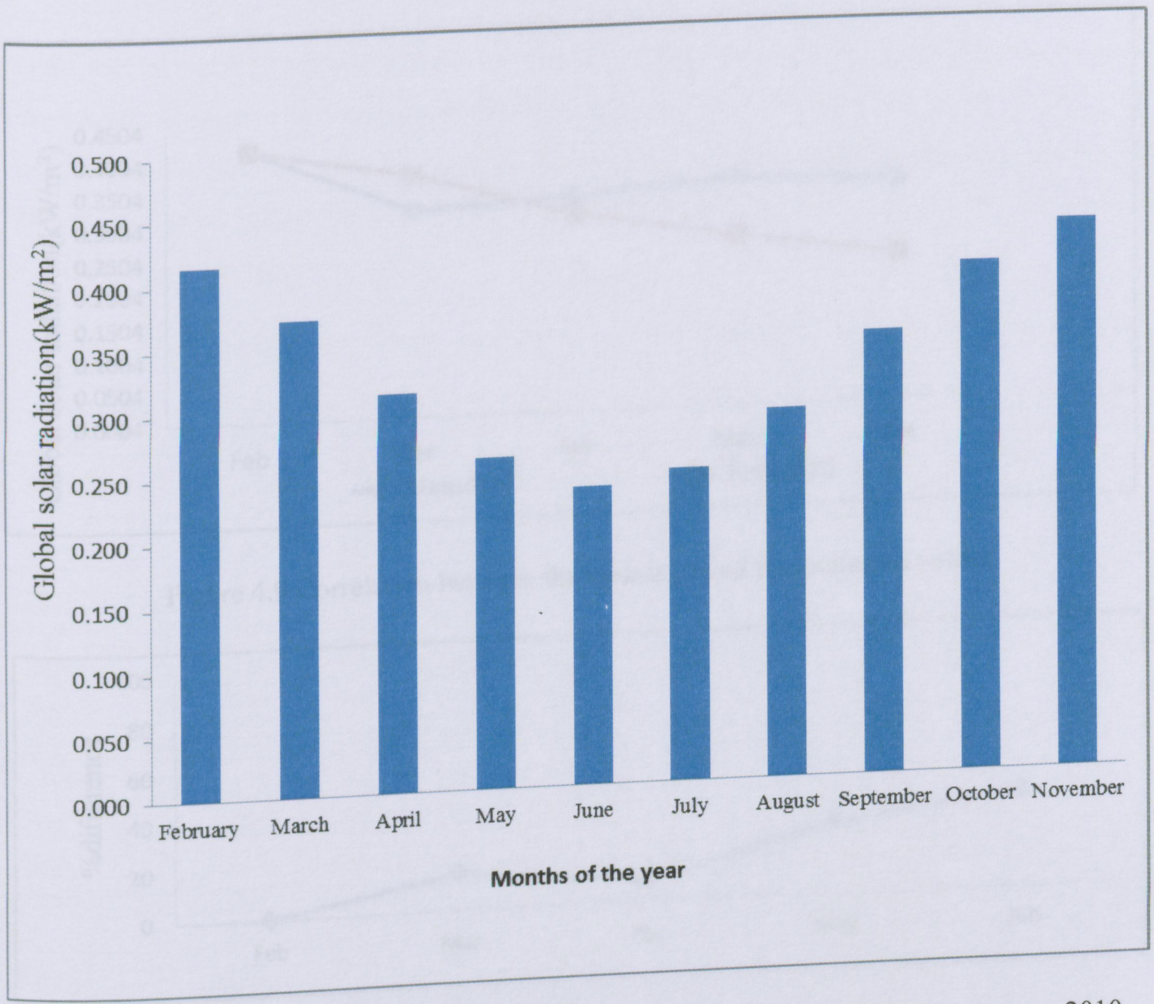

Figure 4.8 Estimated average Monthly global solar radiation for the months of the year 2010

4.1.1.3 Correlation between the measured and estimated global solar radiation

In order to be confident that the estimated values of the global solar radiation are enough to meet the need of the researcher, a correlation graph has been drawn and was depicted in figure 4.9 as one could see from the graph that the two values correspond very well to each other since the percentage differences between each value of the estimated and measured value by the Delta- T data logger are within the range of 0% and 50% for the period of five months. The graph in the figure4.10 showed the percentage difference between the estimated and the measured values. It could be seen in the very same figure 4.10 that the instrument failure has been noted during the month of May 2010.

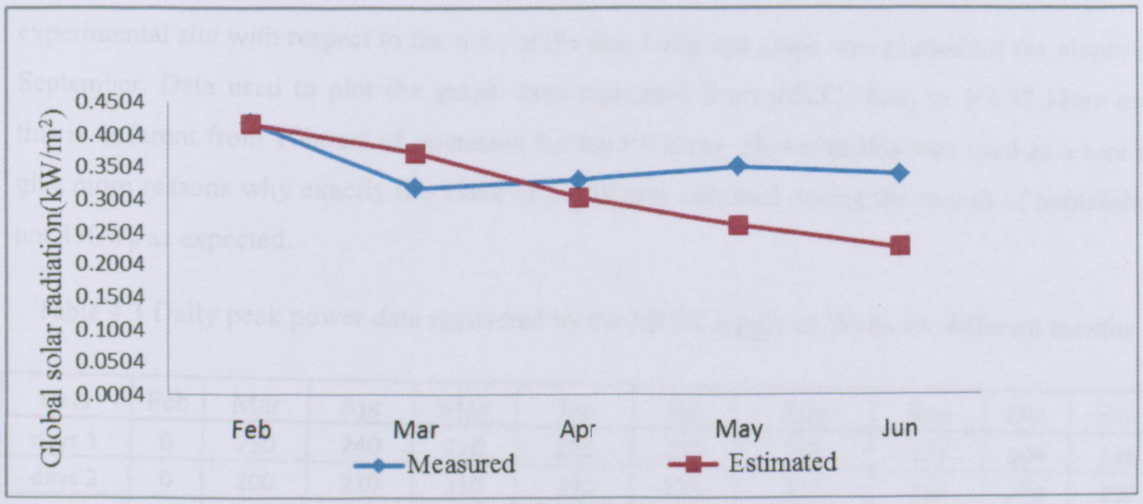

Figure 4.9 Correlation between the measured and the estimated values

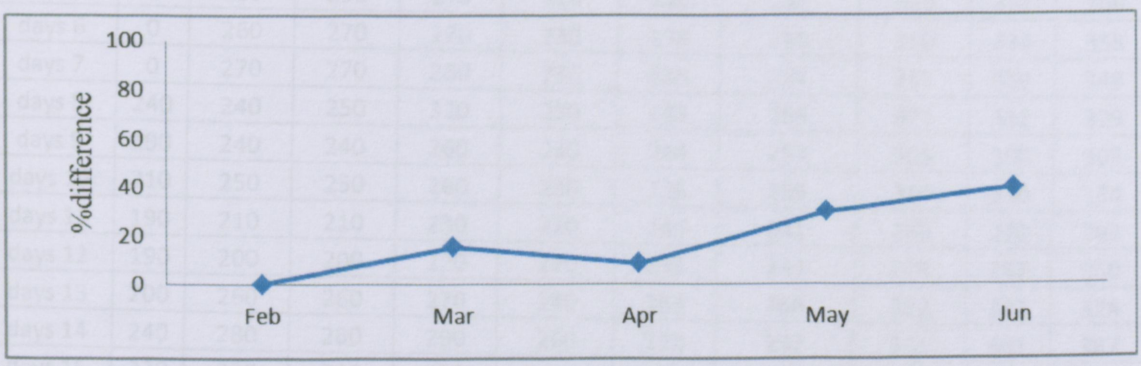

Figure 4.10 The difference between measured and estimated values

4.1.1.4 *Daily peak power measured by the maximum power point tracker (MPPT)*

In this section several graphs of the daily peak power generated by the PV array for the period of nine months were shown. As seen from the graph in figure 4.14, the highest daily average value of the peak power registered by the monitoring instrument for the period of ten hours (10h) from 07h00am to 17h00pm is 372W_p during the months of September 2010. This means that the corresponding daily average value of the electrical energy production registered by the monitoring instrument for the above period of 10h was3.72kWh/day. The value of electrical power can also be confirmed using the vital information of solar radiation intensity falling at the

experimental site with respect to the time of the day. Only one graph was plotted for the month of September. Data used to plot the graph were registered from 08h37:18am to 16h37:18pm and this is different from 10hours of operation for the PV array. However this was used as a tool to give more reasons why exactly the value of $372W_p$was obtained during the month of September not $450W_p$ as expected.

Table 4.3 Daily peak power data registered by the MPPT logger in Watts for different months

Days	Feb	Mar	Apr	May	Jun	Jul	Aug	Sep	Oct	Nov
days 1	0	250	240	220	230	233	253	271	304	318
days 2	0	200	210	210	190	195	215	267	273	290
days 3	0	260	250	270	230	239	258	325	316	328
days 4	0	270	280	280	220	223	241	337	347	349
days 5	0	260	290	270	210	216	225	320	351	369
days 6	0	260	270	270	230	239	249	310	334	358
days 7	0	270	270	280	230	235	257	333	339	348
days 8	240	240	250	320	230	243	256	372	312	329
days 9	190	240	240	260	230	244	253	305	300	309
days 10	210	250	250	260	230	236	259	310	310	334
days 11	190	210	210	230	220	244	241	289	270	293
days 12	190	200	200	220	220	233	244	274	267	260
days 13	200	260	260	270	240	263	266	322	327	324
days 14	240	280	280	290	260	272	287	341	341	367
days 15	270	230	240	250	260	263	276	301	307	327
days 16	190	230	230	250	260	269	290	307	296	310
days 17	220	200	220	220	240	248	263	278	285	309
days 18	260	270	270	280	270	275	296	337	336	339
days 19	270	210	210	230	260	267.5	287	287	273	289
days 20	190	230	230	250	260	265	290	309	299	305
days 21	280	140	150	180	250	255	292	229	208	238
days 22	260	290	280	270	250	259	298	328	336	365
days 23	260	220	220	260	260	265	306	319	279	306
days 24	260	250	250	260	260	270	304	320	309	334
days 25	230	240	250	250	250	256	275	308	303	336
days 26	240	190	250	210	250	261	270	268	319	339
days 27	240	200	230	210	250	255	270	260	298	314
days 28	250	190	210	210	210	222	234	269	279	296
days 29	0	270	270	250	250	255	289	307	330	357
days 30	0	220	230	210	210	223	259	266	296	318
days 31	0	300	0	270	0	257	278	0	280	0

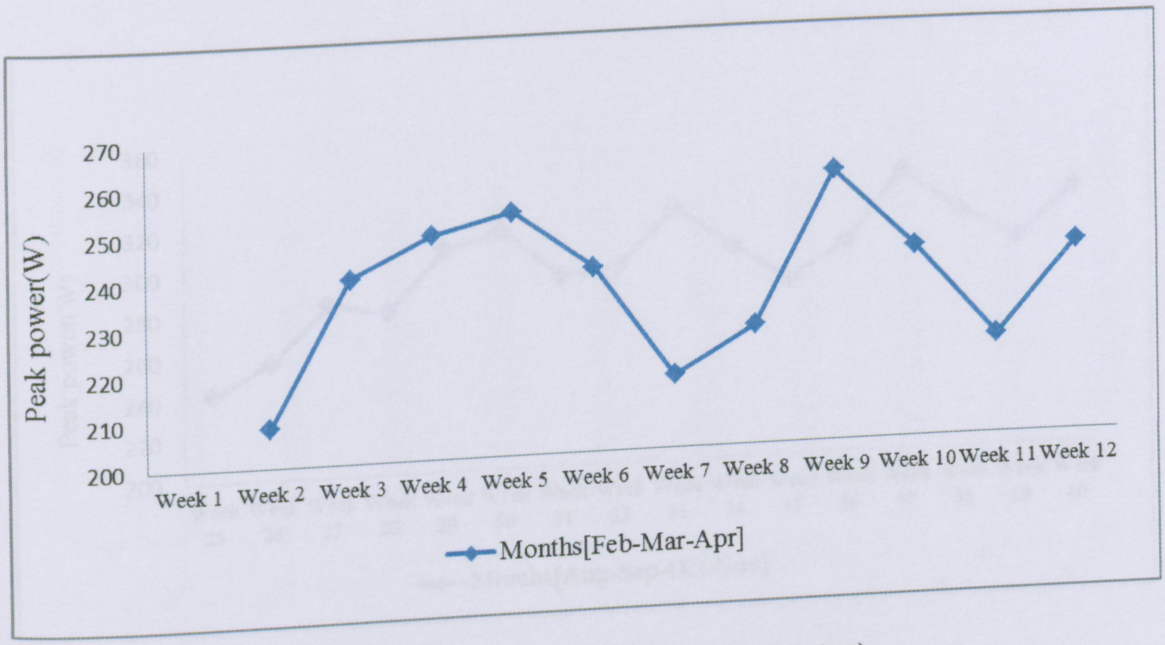

Figure 4.11 Peak power for the months (Feb-Mar-Apr)

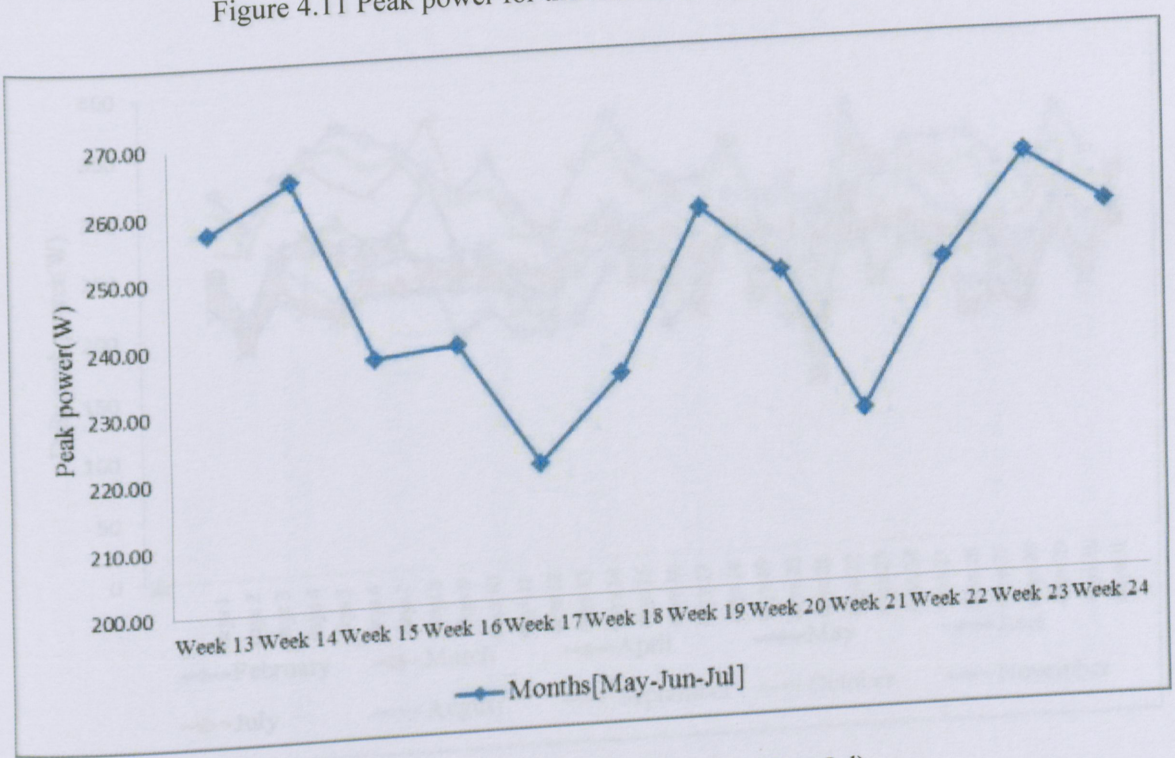

Figure 4.12 Peak power for the months (May-Jun-Jul)

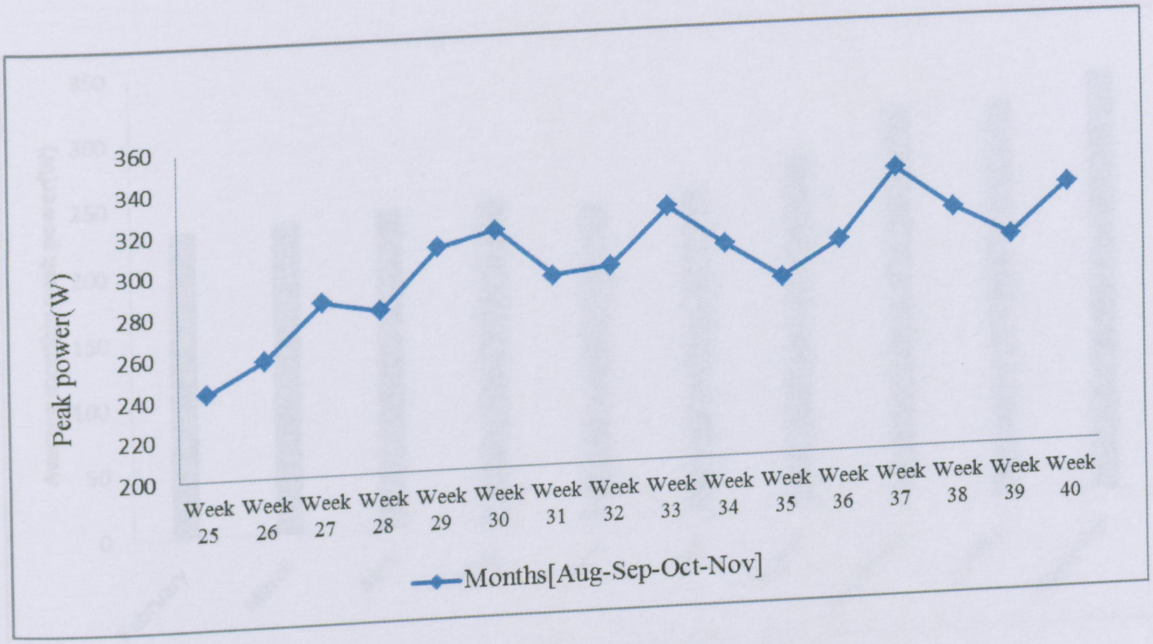

Figure 4.13 Peak power for the months (Aug-Sep-Oct)

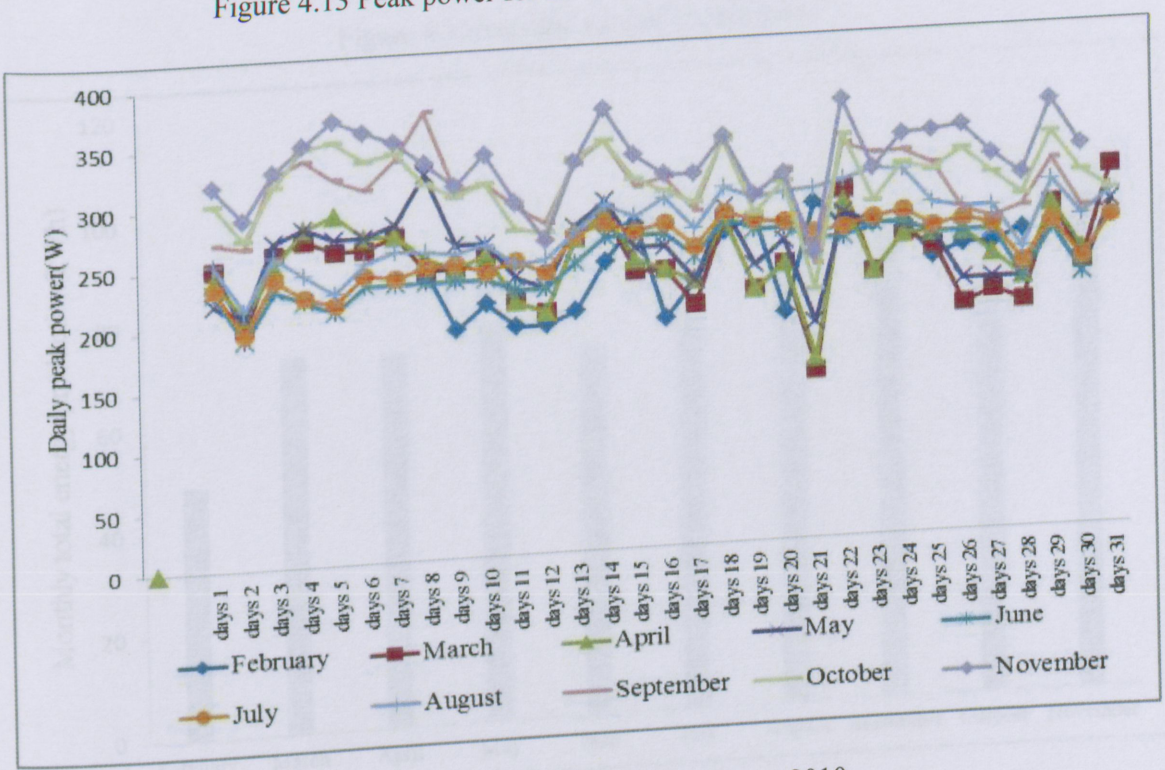

Figure 4.14 Monthly peak power for the year 2010

Figure 4.15Average monthly peak power

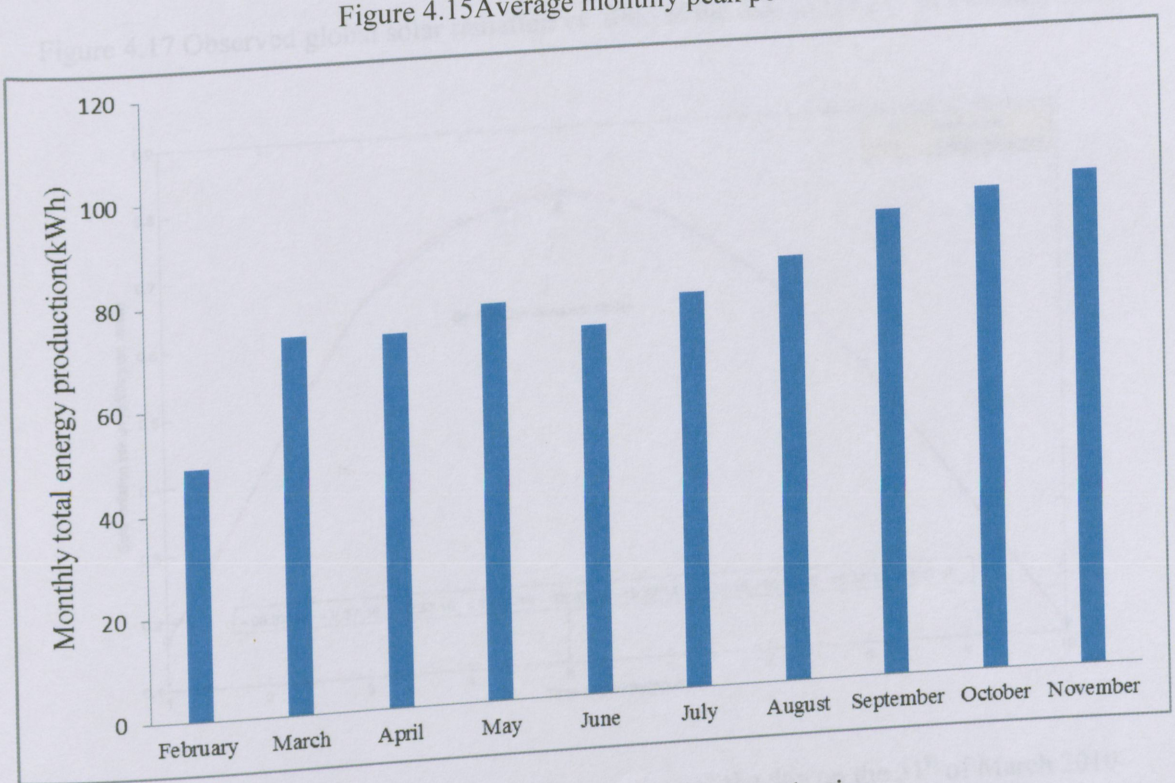

Figure 4.16 Monthly total electrical energy production

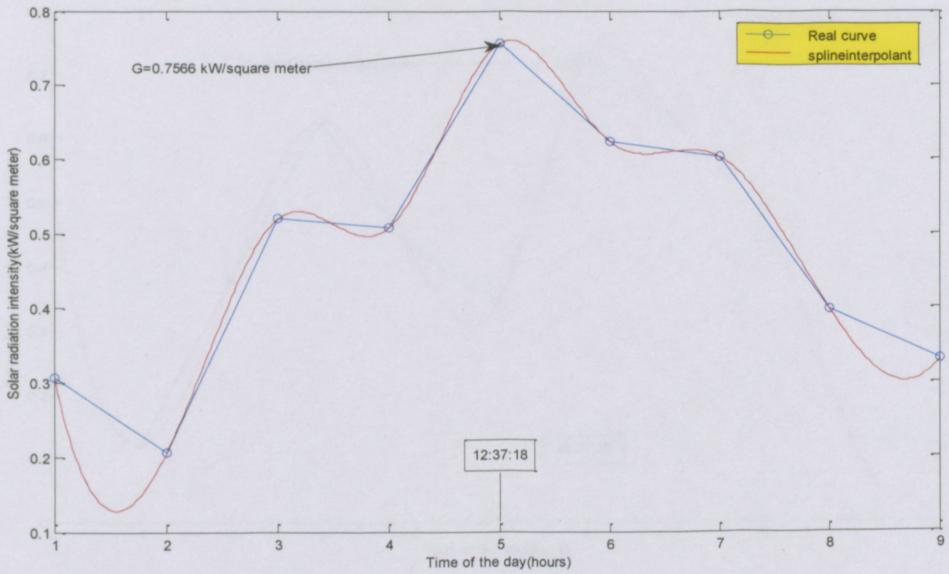

Figure 4.17 Observed global solar radiation vs. time of the day on the 21st of February 2010

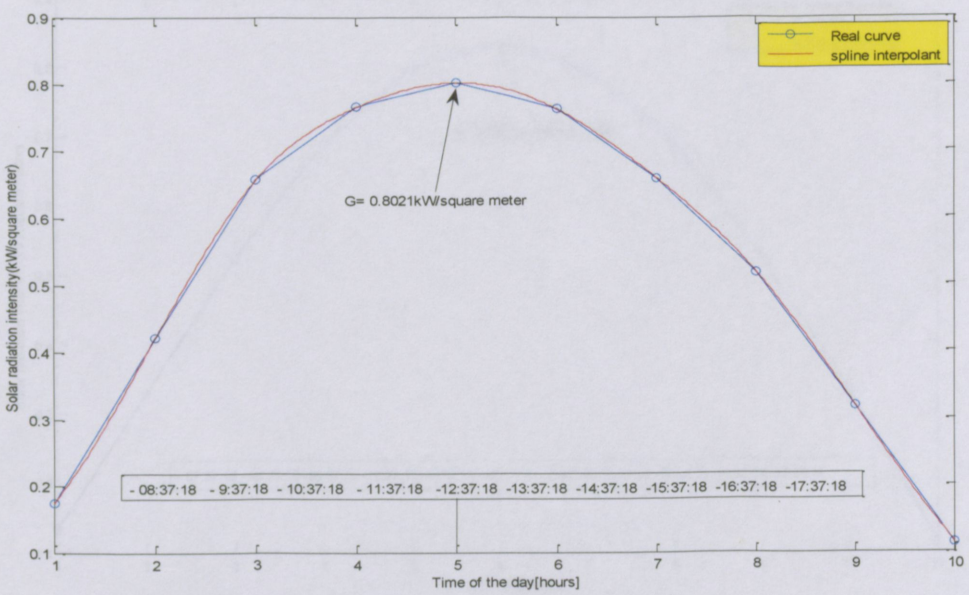

Figure 4.18 Observed global solar radiation vs. time of the day on the 31st of March 2010

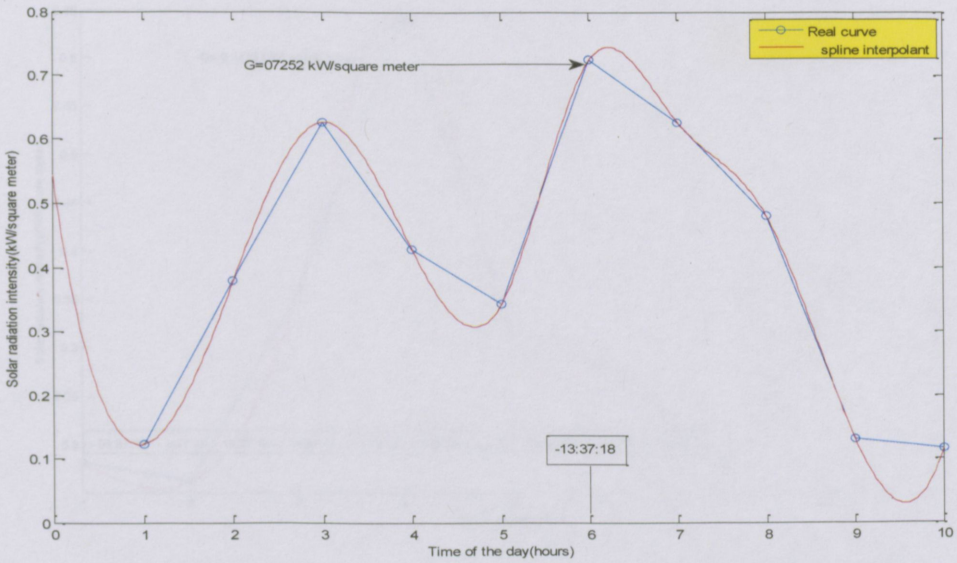

Figure 4.19 Observed global solar radiation vs. time of the day on the 5th of April 2010

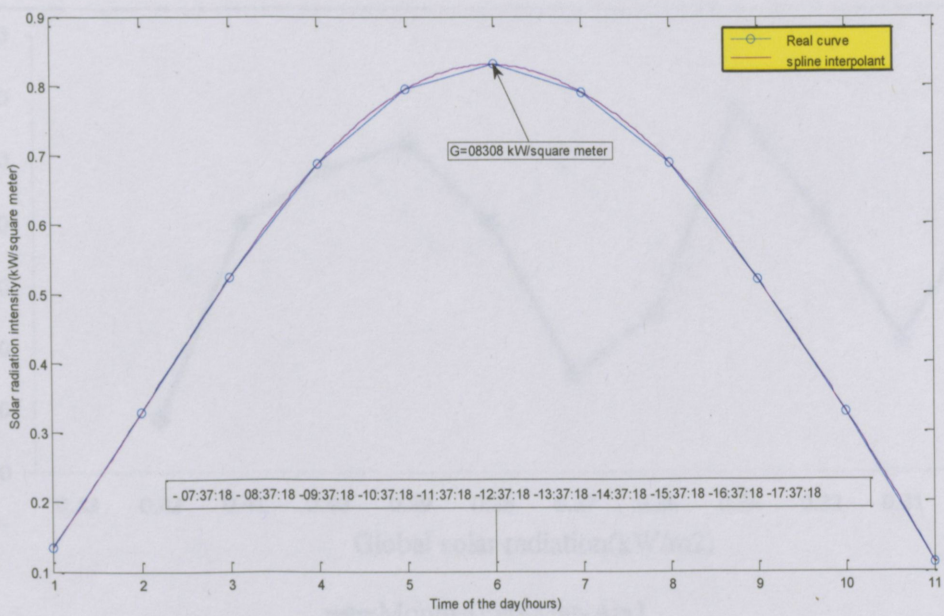

Figure 4.20 Observed global solar radiation vs. time of the day on the 21st of May2010

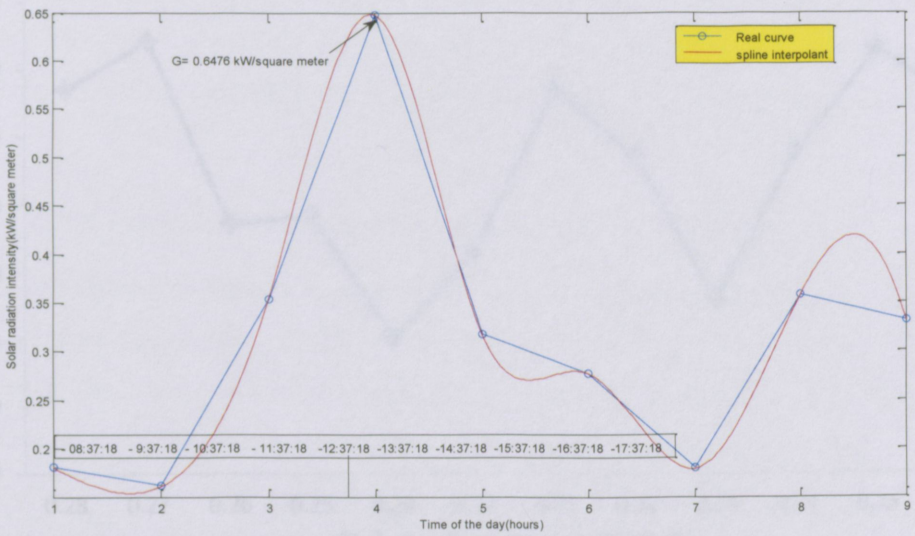

Figure 4.21Observed global solar radiation vs. time of the day on the 24th of June 2010

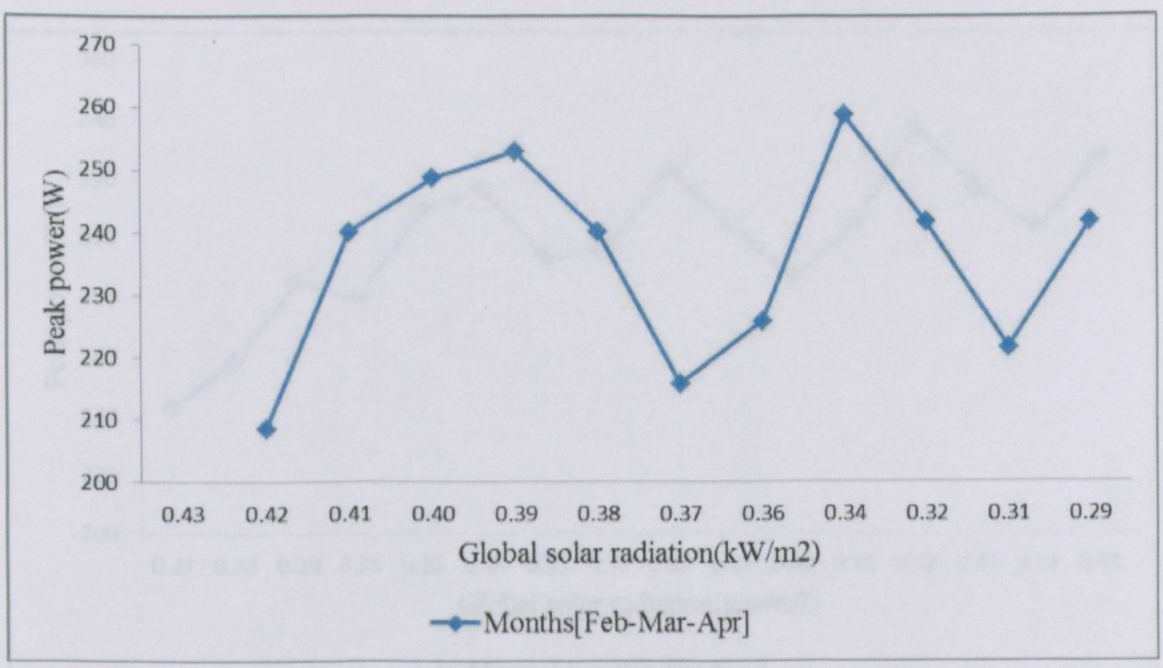

Figure 4.22 Peak power vs. estimated global solar radiation

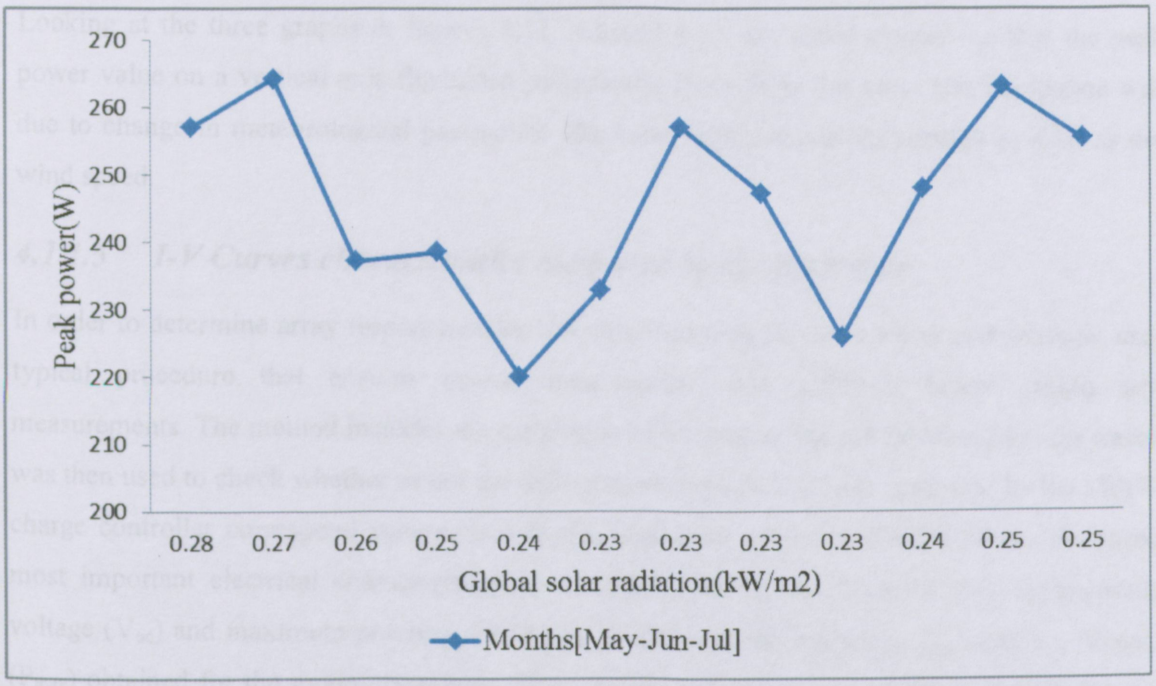

Figure 4.23 Peak power vs. estimated global solar radiation

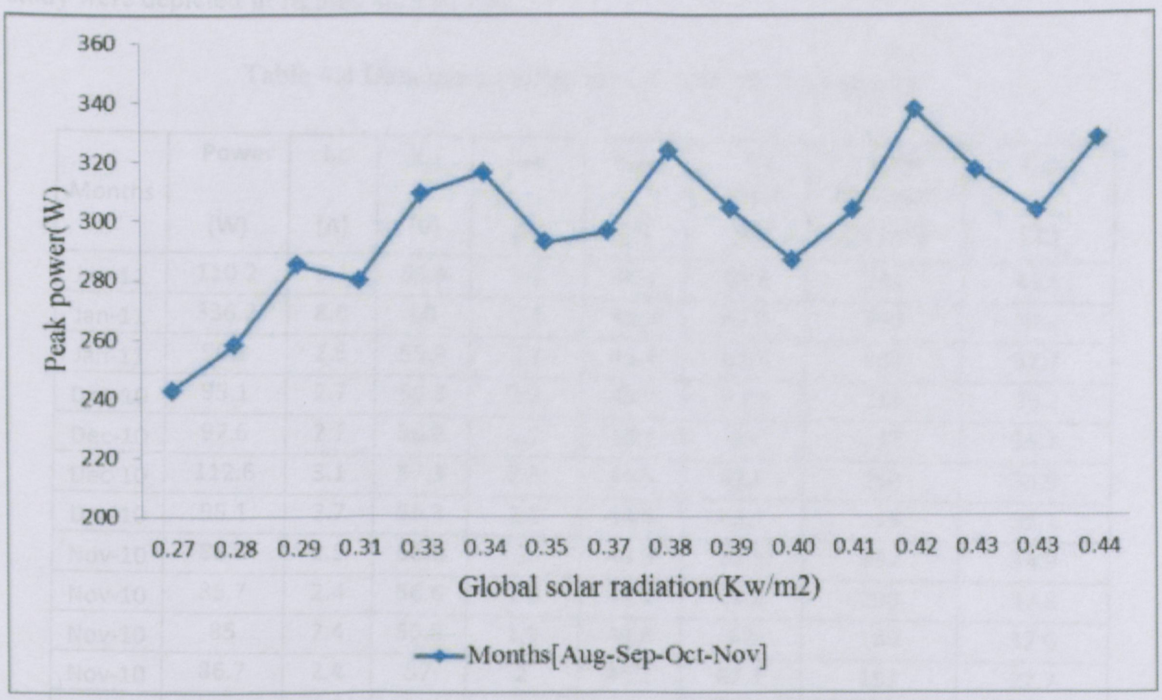

Figure 4.24 Peak power vs. estimate global solar radiation

Looking at the three graphs in figures 4.11, 4.12and 4.13 one could closely see that the peak power value on a vertical axis fluctuated periodically throughout the year. The fluctuation was due to change in meteorological parameters like solar radiation, air temperature as well as the wind speed.

4.1.1.5 I-V Curves characteristics measured by the DS tracer

In order to determine array response under real conditions, an IV curve tracer was of major use, typical procedure that ensures quality measurement was followed before taking any measurements. The method includes the calibration of the tracer. The information from the tracer was then used to check whether or not the daily accumulated peak power measured by the MPPT charge controller correspond very well with the rated peak power of the PV panel. The three most important electrical characteristics of a module are the short-current (I_{sc}), open-circuit voltage (V_{oc}) and maximum power point (P_{max}). In table 4.4 the values I_{sc}, I_{peak} and V_{oc}, Vpeak (P_{max}) obtained for the mono-crystalline silicon panels at 12H03were presented. Sample curves (four for each week of the month except for the month of January 2011) obtained in the present study were depicted in figures 4.25 to 4.47.

Table 4.4 Data measured by the DS 100C IV curve tracer

Months	Power (W)	I_{sc} (A)	V_{oc} (V)	I_{peak} (A)	V_{peak} (V)	Fill Factor (%)	Solar Radiation (W/m^2)	T_{Cell} (^0C)
Jan-11	110.2	3.1	55.9	2.5	44.1	63.5	246	41.6
Jan-11	336.2	8.8	60	7.4	45.5	63.9	750	39.4
Jan-11	90.9	2.6	55.9	2.1	43.4	62.8	202	37.7
Dec-10	95.1	2.7	56.3	2.2	43.7	62.9	211	36.2
Dec-10	97.6	2.7	56.6	2.2	44.1	63	217	35.7
Dec-10	112.6	3.1	57.3	2.5	44.5	63.6	250	35.9
Dec-10	98.1	2.7	56.8	2.2	44.5	63.1	218	35.1
Nov-10	88.6	2.5	56.6	2	43.6	62.5	197	34.9
Nov-10	85.7	2.4	56.6	1.9	44.1	62.2	190	33.8
Nov-10	85	2.4	56.8	1.9	43.6	62	189	32.6
Nov-10	86.7	2.4	57	2	44.1	62.1	192	32.7
Oct-10	87.9	2.5	57.3	2	44.2	62.1	195	31.8
Oct-10	86.9	2.4	57.3	1.9	44.7	62	193	32.2
Oct-10	86.5	2.4	57.3	1.9	44.7	62.1	192	31.7

Oct-10	87.2	2.4	57.3	2	44.7	62.2	193	31.6
Sep-10	87	2.4	57.5	1.9	44.7	62.1	193	30.8
Sep-10	86.4	2.4	57.5	2	44	62.1	192	30.5
Sep-10	85.9	2.4	57.5	1.9	44.2	61.9	191	30.9
Sep-10	85.9	2.4	57.5	1.9	44.7	61.9	190	30.4
Aug-10	83.4	2.4	57.5	1.9	44.2	61.7	185	30.5
Aug-10	81.7	2.3	57.5	1.8	44.9	61.5	181	30.3
Aug-10	81.7	2.3	57.5	1.8	44.6	61.7	181	29.3
Aug-10	82	2.3	57.5	1.9	44.1	61.8	182	29.5
Jul-10	84.6	2.4	57.7	1.9	45.3	61.9	188	29.8
Jul-10	88.4	2.5	58	2	45.3	62.1	196	29.9
Jul-10	89.8	2.5	58	2	44.8	62.1	199	30.1
Jul-10	93.9	2.6	58.2	2.1	44.7	62.2	208	30.1
Jun-10	95.4	2.6	58.3	2.1	45.2	62.3	212	29.6
Jun-10	98	2.7	58.5	2.2	45.4	62.3	217	29.6
Jun-10	144.9	3.8	59.8	3.1	47.1	64	322	29.9
Jun-10	117.9	3.1	58.8	2.6	45.4	63.7	262	30.8
May-10	131.8	3.5	59.3	2.8	46.7	64.2	293	30.8
May-10	178.1	4.5	60.3	3.8	47	65	396	31.9
May-10	331.6	8.3	61.7	7	47.3	64.4	737	33.1
May-10	441.3	11.3	62	9.5	46.6	63.3	982	35.2
Apr-10	347.4	9	60.8	7.6	45.7	63.8	775	39.3
Apr-10	104.3	3	56.2	2.4	43.3	62.8	232	40.2
Apr-10	103.8	2.9	56.4	2.4	43.3	62.5	231	40.1
Apr-10	385.2	10.5	58.8	8.9	43.4	62.2	865	48.9
Mar-10	397.8	10.9	58.8	9.2	43.4	62	893	48.5
Mar-10	400.2	11	58.8	9.3	43	61.8	899	49.2
Mar-10	399.9	11	58.6	9.3	43.2	61.9	899	49.8
Mar-10	399.1	11	58.6	9.3	43	61.7	897	50.4
Feb-10	398.7	11.1	58.5	9.3	42.8	61.7	897	50.7
Feb-10	398.8	11.1	58.3	9.3	42.8	61.6	898	51.6
Feb-10	399.5	11.2	58.3	9.3	42.8	61.5	900	51.9
Feb-10	272.9	11	58.2	6.7	40.6	42.6	614	51.1

The peak power output of the PV array depends mainly on the amount of radiation quantities striking on its front surface, which in this study was not horizontal. As mentioned in chapter 2 of this research project, radiation quantities may be classified into two groups according to origin: solar radiation and terrestrial radiation.

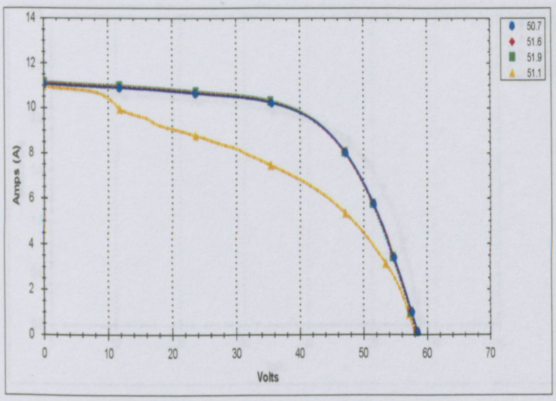

Figure 4.25 I-V Curves during February2010

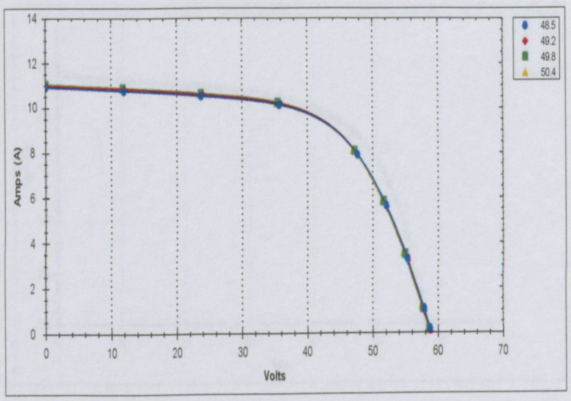

Figure 4.26 I-V Curves during March 2010

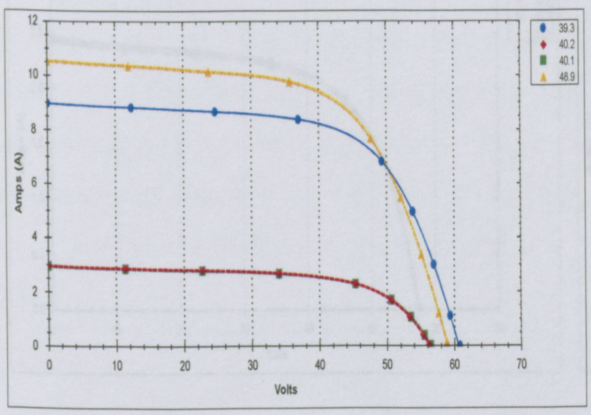

Figure 4.27 I-V Curves during April 2010

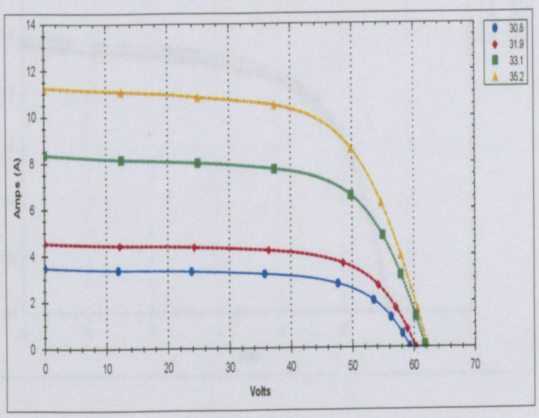

Figure 4.28 I-V Curves during May 2010

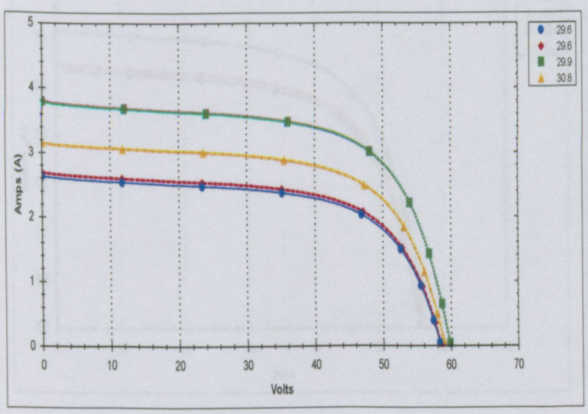

Figure 4.29 I-V Curves during June 2010

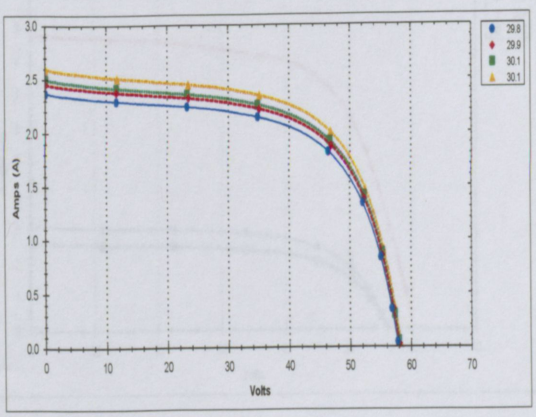

Figure 4.30 I-V Curves during July 2010

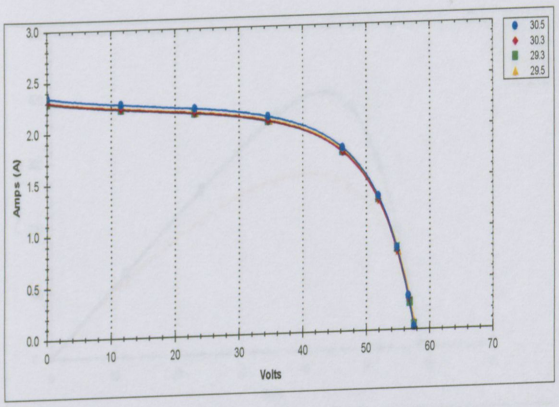

Figure 4.31 I-V Curves during August 2010

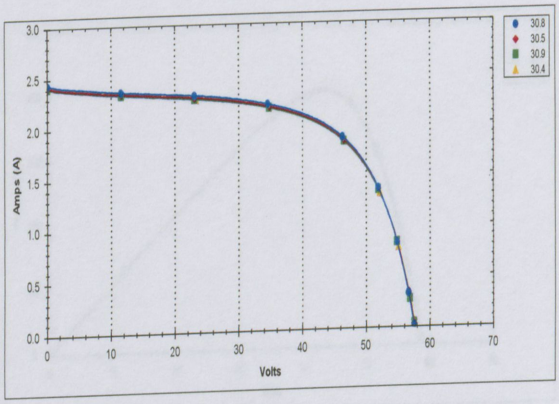

Figure 4.32 I-V Curves during September 2010

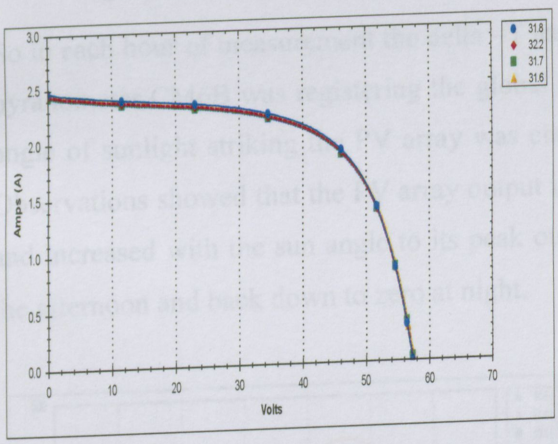

Figure 4.33 I-V Curves during October 2010

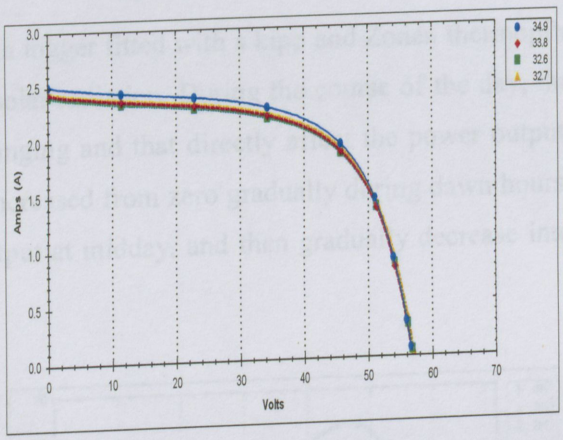

Figure 4.34 I-V Curves during November 2010

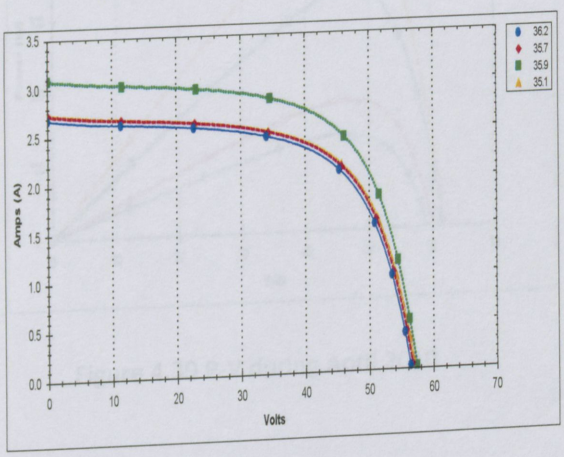

Figure 4.35 I-V Curves during December 2010

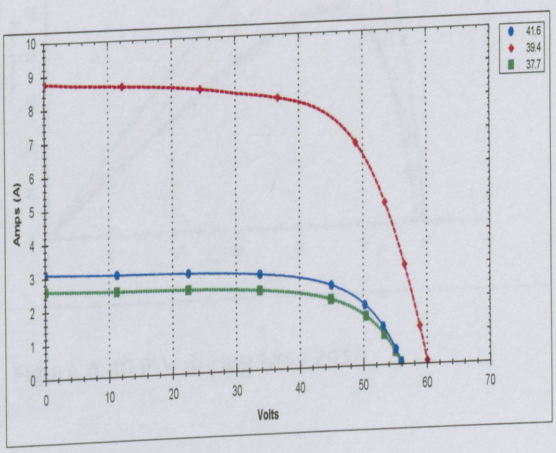

Figure 4.36 I-V Curves during January 2010

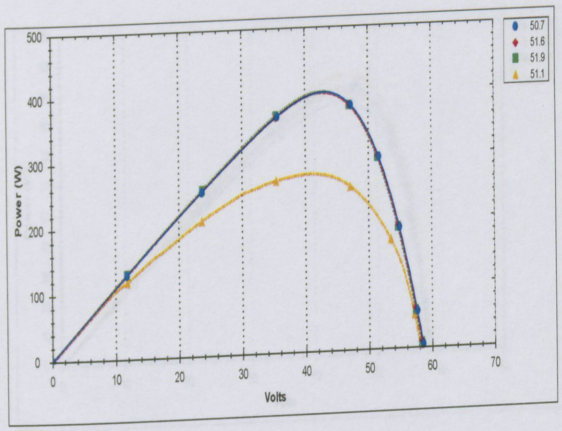

Figure 4.37 P-V during February 2010

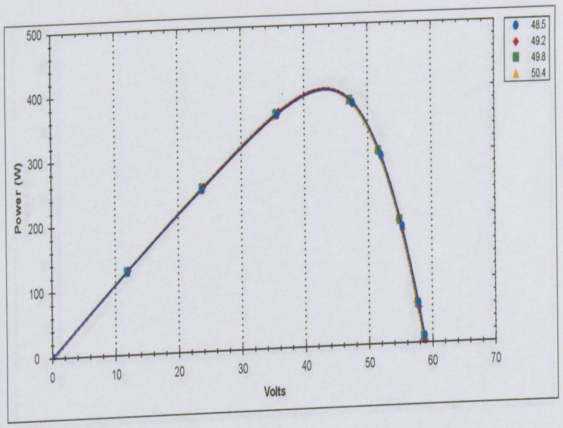

Figure 4.38 P-V during March 2010

So in each hour of measurement the delta –T data logger fitted with a kipp and Zonen thermopile pyranometer CM6B was registering the global solar radiation. During the course of the day, the angle of sunlight striking the PV array was changing and that directly affect the power output. Observations showed that the PV array output increased from zero gradually during dawn hours, and increased with the sun angle to its peak output at midday, and then gradually decrease into the afternoon and back down to zero at night.

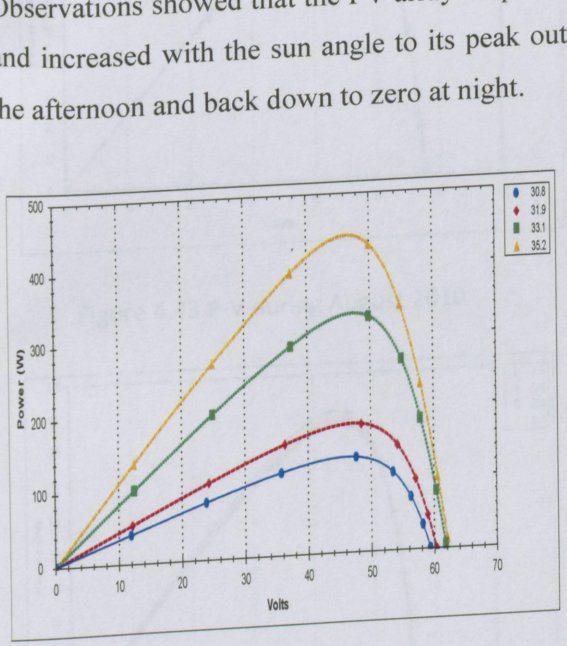

Figure 4.39 P-V during April 2010

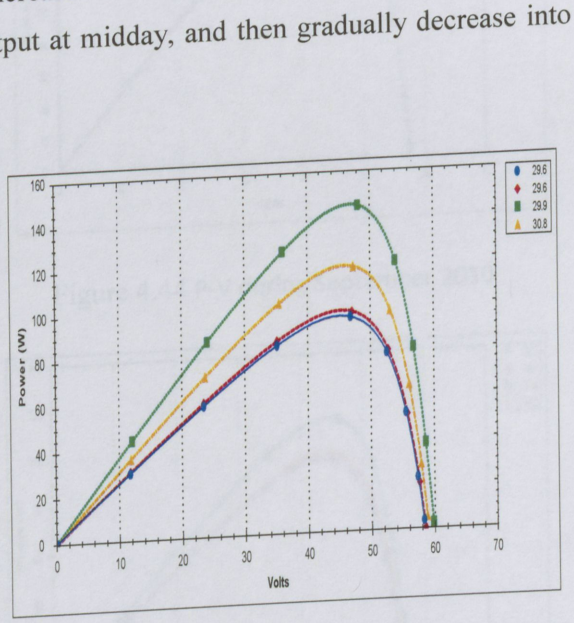

Figure 4.40 P-V during May 2010

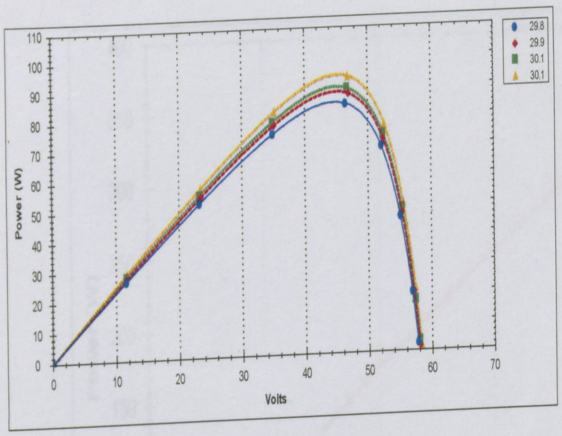

Figure 4.41 P-V during June 2010

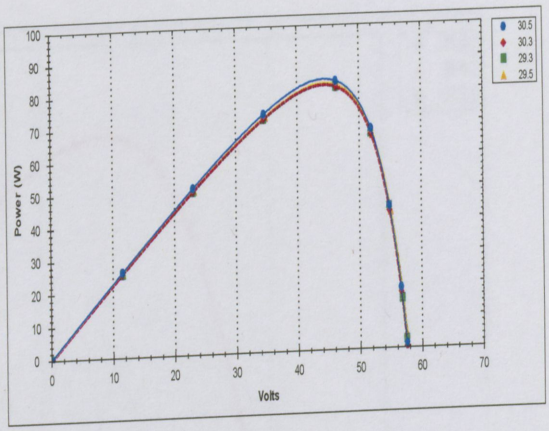

Figure 4.42 P-V during July 2010

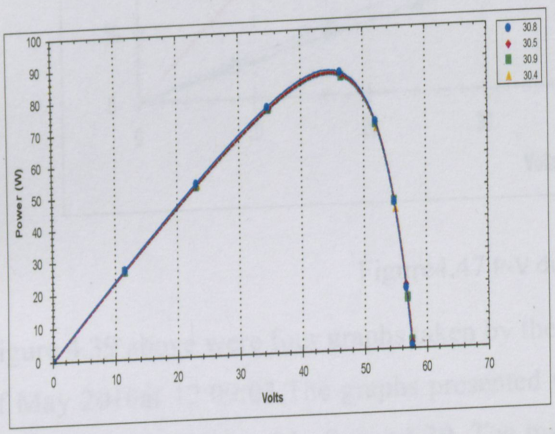

Figure 4.43 P-V during August 2010

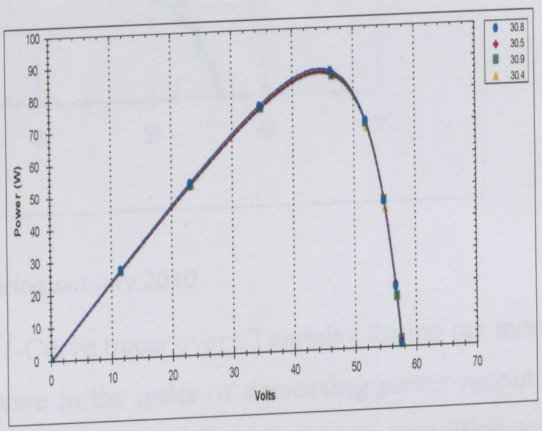

Figure 4.44 P-V during September 2010

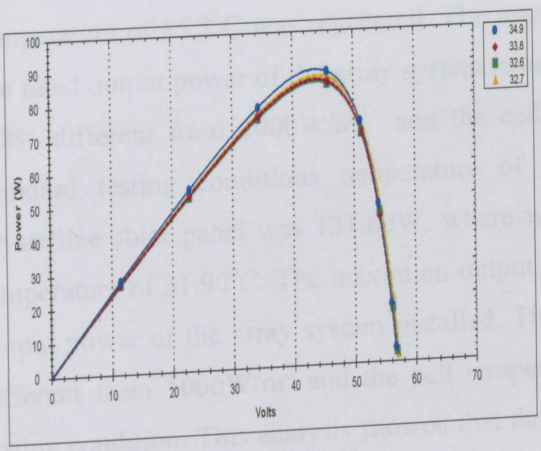

Figure 4.45 P-V during October 2010

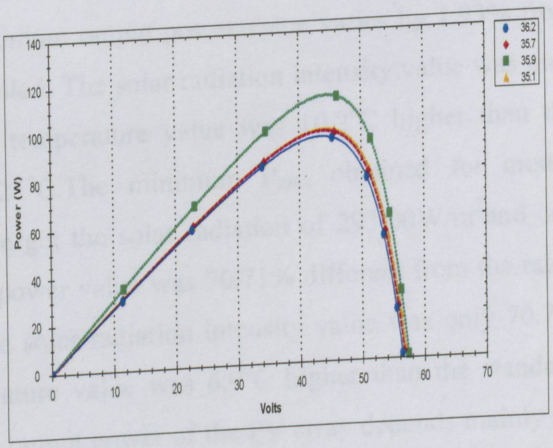

Figure4.46 P-V during November 2010

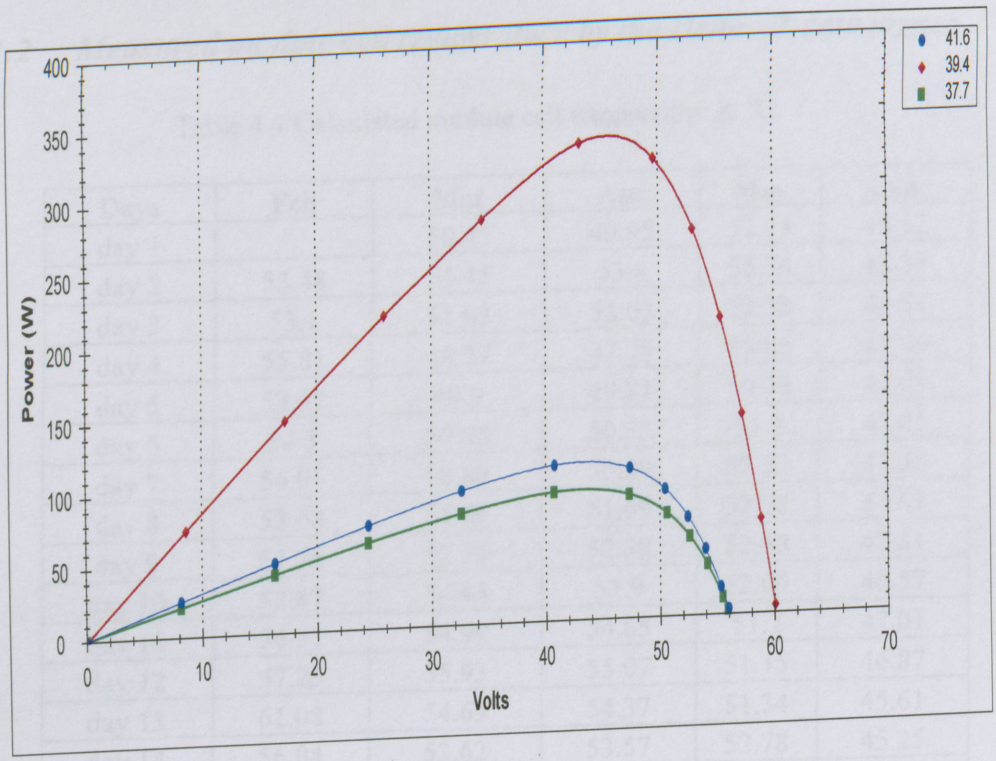

Figure4.47 P-V during January 2010

Figure 4.39 above were four graphs taken by the I-Curve tracer every Thursday during the month of May 2010at 12:09:03.The graphs presented were in the order of decreasing power output of the PV array as depicted in figure 4.39. The maximum P_{max} obtained for mono-crystalline solar panel was 441.30 W, when the maximum solar radiation intensity of 982.0 $W/m^2$and cell temperature of 35.2°C was registered. The maximum output power value varies by 1.93% from the rated output power of the array system installed. The solar radiation intensity value was only 1.8% different from $1000W/m^2$ and the cell temperature value was 10.2°C higher than the standard testing conditions temperature of 25°C.The minimum P_{max} obtained for mono-crystalline solar panel was 131.80W, where we get the solar radiation of $293.00W/m^2$and cell temperature of 31.90°C. The maximum output power value was 70.71% different from the rated output power of the array system installed. The solar radiation intensity value was only 70.7% different from $1000W/m^2$ and the cell temperature value was 6.9°C higher than the standard testing condition. This analysis showed that the output power of the PV array depends mainly on the solar radiation intensity. Some of the factors that lowered the output power were cloud transitions.

4.1.1.2 *Measured module cell temperature by the Delta –T data logger*

Table 4.4 Calculated module cell temperature in °C

Days	Feb	Mar	Apr	May	Jun
day 1		50.45	49.95	52.78	48.12
day 2	53.48	54.45	53.8	55.74	46.35
day 3	53.1	51.02	51.02	52.53	46.57
day 4	55.81	48.27	47.79	49.86	47.46
day 5	53.37	49.9	49.81	50.75	47.01
day 6	54.3	50.06	50.33	51.2	47.01
day 7	56.01	50.86	50.89	52.23	47.38
day 8	53.68	51.66	51.69	52.28	47.67
day 9	51.78	52.79	52.39	52.48	47.31
day 10	52.87	54.44	53.9	52.09	46.57
day 11	56.51	54.99	54.65	51.2	47.01
day 12	57.23	55.93	55.07	51.15	46.87
day 13	61.08	54.63	54.37	51.34	45.61
day 14	56.04	53.62	53.57	52.78	45.25
day 15	53.16	49.43	50.42	50.31	44.29
day 16	53.9	51.85	51.85	51.85	44.8
day 17		54.96	54.65	51.2	45.54
day 18	48.71	49.66	50.19	48.77	45.99
day 19	50.62	51.02	51.02	51.02	44.14
day 20	48.99	53.35	53.15	53.35	44.59
day 21	51.19	46.72	47.7	47.93	43.55
day 22	52.28	49.58	49.91	48.92	44.44
day 23	51.95	51.89	51.69	50.11	44.66
day 24	51.71	51.92	52.11	52.63	45.61
day 25	51.75	54.68	54.55	53.37	45.61
day 26	53.19	56.17	55.31	56.48	47.31
day 27	50.29	55.95	55.12	55.84	47.16
day 28	50.93	55.87	55.4	55.45	55.45
day 29		48.96	49.15	49.86	49.86
day 30		54.84	54.6	53.22	53.22
day 31				50.8	

The cell temperature data was calculated from the ambient temperature data measured of the period of five month by the Delta-T data logger. The equation used to calculate the cell temperature is given by the

$$T_{cell} = T_{ambient} + (Noct - 20\,^{O}C) \quad (4.1)$$

Where, the meaning of the symbols are as defined in chapter 3

The temperature of the PV array cells was also important when computing the power output of the PV array. The PV cell temperature was the measured temperature of the rear surface of the PV array. Two modes for calculating the rear surface of the PV array cell temperature were applied. One assumed that the cell temperature was isolated. The other assumed that cell temperature was at the outdoor air temperature.

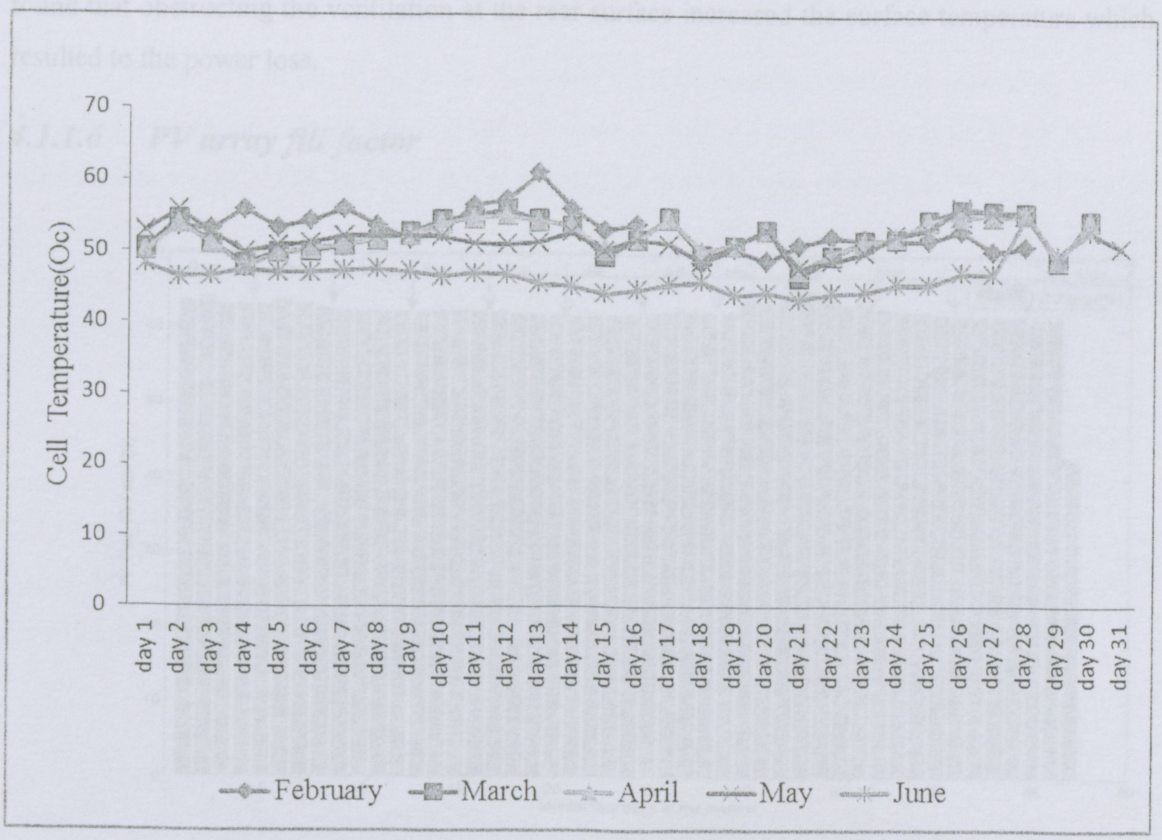

Figure4.48 Calculated Cell temperatures from the ambient temperature values

The performance of an array of identical modules was assumed to be linear with the number of modules in series and parallel. It was found that cell temperature increase of 10°C from STC Cell temperature of 25°C led to a power loss of about 5%, meaning that a 450W installed PV array produces 450 W at STC and 422.5 W at 35°C.This is true only if the solar radiation intensity striking each of the photovoltaic cells is close to $1000Wm^2$.

During the night the cell temperature was less the same as the ambient air temperature, but in clear sky days the cell temperature exceeded the ambient air temperature by 30°C and higher. The temperature of the rear surface of the PV array was noted to be higher than the temperature of the front surface of the PV array where the incident solar radiation intensity strikes. This was not surprisingly because the front surface was a glass surface. It was found that after five months of installation, some of the PV array cells were found turning blue in colour from their original black colour as they were before the long term exposure to the solar radiation intensity. It was found that obstructing the ventilation at the rear surface increased the surface temperature which resulted to the power loss.

4.1.1.6 PV array fill factor

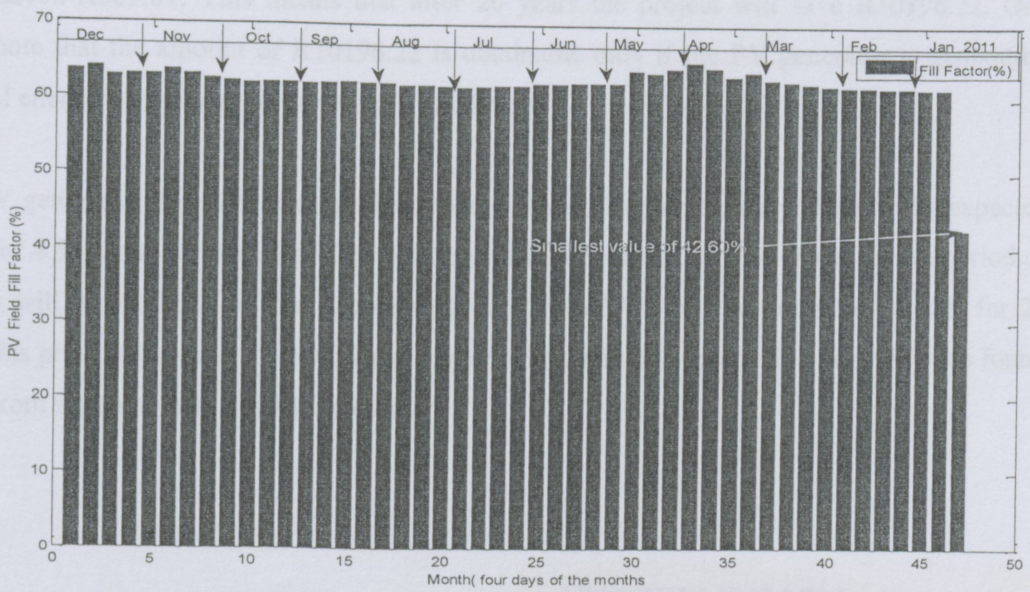

Figure 4.49 Fill factor for the months of Feb2010-January 2011

As discussed in chapter 2, the main impact of series resistance is to reduce the fill factor (*FF*), although noticeably high values may also reduce the short-circuit current (I_{sc}). The effect of the series resistance on the I-V curve were shown (yellow curve) in the figure 4.49with the value of the fill factor of 42.60% and the short circuit current value of 11 Amps. That value of *FF* was the only smallest value obtained throughout the whole measurements. The percentage difference between the STC value (FF_{STC}=72%) and field test value of (*FF*=42.60%) was 40.83%.

The calculated series resistance of the PV array system was found to be equal 7.5278 Ohms. The impairment that reduced the fill factor also reduced the maximum power output by reducing I_{mp} and V_{mp}. See the P-V curve above in figure 4.50 for the months of January 2011. The above findings proved the fact that the series resistance has a significant effect on the performance of the PV module.

4.1.1.7 Electrical energy saving analysis

Looking at the table in figure 4.3 the annual monthly total electrical energy generated by a 450W PV array system was784.325kWh. If Eskom scale of selling electrical energy in South Africa is used in this project as to see how much the project is saving per month, one will find that the project saved R509.81. This means that after 20 years the project will save R10196.22. One should note that the amount of R10196.22 is obtainable only if the PV generator is generating electrical energy which is approximately 3.72kWh/day.

If the PV generator generates the electrical energy which is approximately close to the expected amount of 4.5kW for the period of 10h then the total amount that will be saved for the period of 20 years will be R21060.00. The Eskom scale of R0.65c/kWh will not remain like this for 20 years. This price will rise to R3.00/kWh or higher. The data table depicted in table 4.5 was found from Eskom inclining block tariff structure.

Table 4.5 Comparison of monthly amount (excluding VAT) payable under the inclining block tariff Structure

Average monthly usage	50 kWh	150kWh	350 kWh	600 kWh	1000 kWh	1500 kWh	5000 kWh
Amount Payable in2010/11	R 27.35	R 85.83	R 202.79	R 393.67	R 728.63	R 1,147.33	R 4,078.23
Amount Payable in2011/12	R 28.83	R 94.99	R 227.31	R 467.43	R 888.83	R 1,415.58	R 5,102.83
R/month increase	R 1.48	R 9.16	R 24.52	R 73.77	R 160.21	R 268.26	R 1,024.61
% increase	5.39%	10.67%	12.09%	18.74%	21.99%	23.38%	25.12%

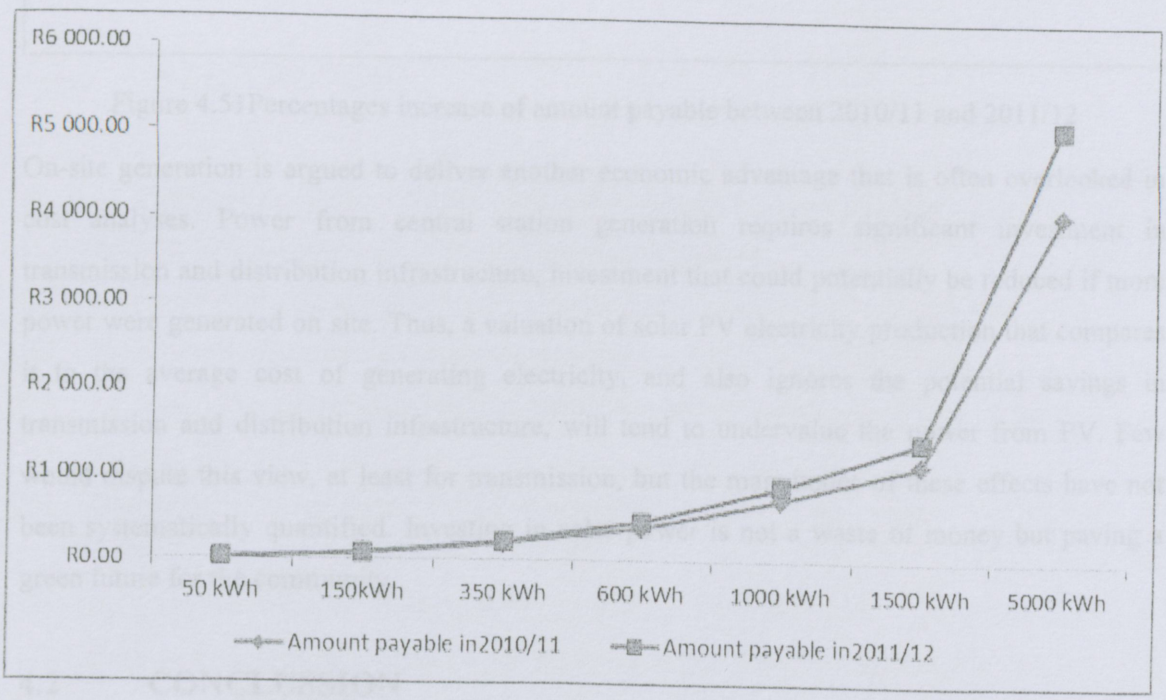

Figure 4.50 Comparison of monthly amount (excluding VAT) payable under the inclining block tariff structure

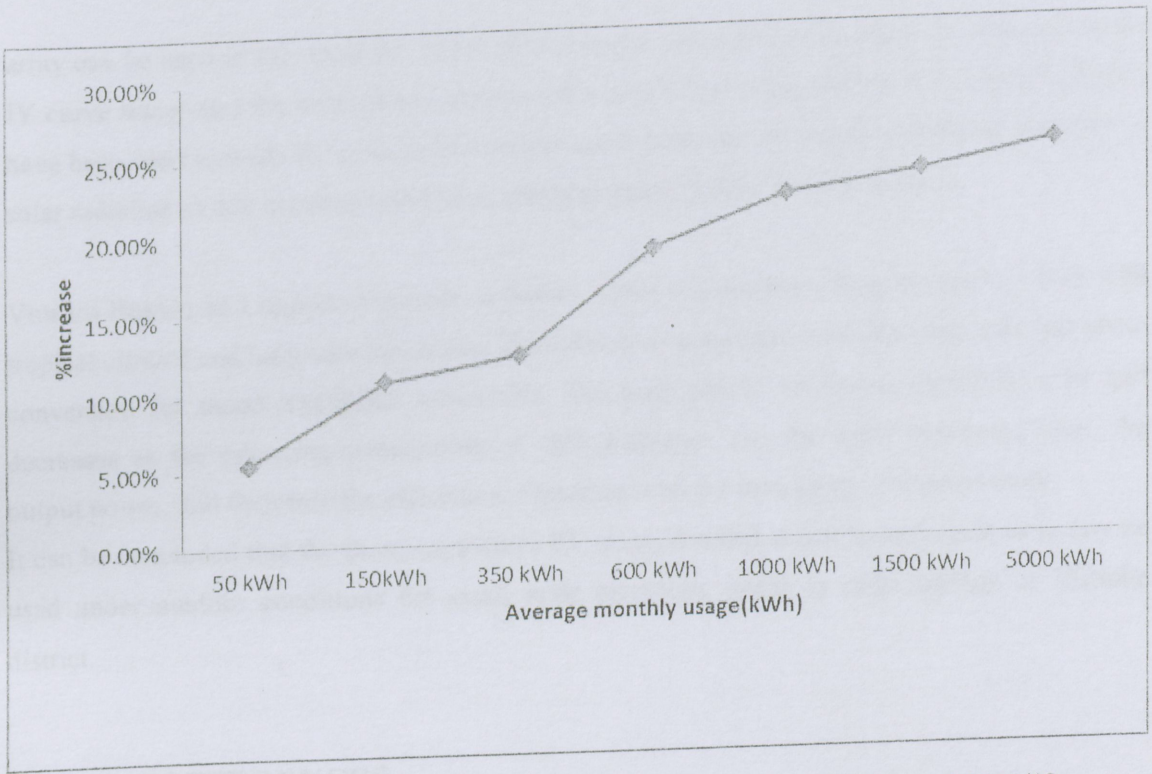

Figure 4.51Percentages increase of amount payable between 2010/11 and 2011/12

On-site generation is argued to deliver another economic advantage that is often overlooked in cost analyses. Power from central station generation requires significant investment in transmission and distribution infrastructure, investment that could potentially be reduced if more power were generated on site. Thus, a valuation of solar PV electricity production that compares it to the average cost of generating electricity, and also ignores the potential savings in transmission and distribution infrastructure, will tend to undervalue the power from PV. Few would dispute this view, at least for transmission, but the magnitudes of these effects have not been systematically quantified. Investing in solar power is not a waste of money but paving a green future for the community.

4.2 CONCLUSSION

The conclusion based on the peak power study shows that the rated value of the peak power of a PV array is in close comparison with the observed value. From the experiment a difference of 2% was noted during the monitoring period. This implies that the output harnessed from the PV

array can be used in this location. Some of the results obtained in this study are tested using the IV curve tracer and the comparison is reasonably good. The estimated values of solar radiation have been used to study the peak power performance; however the experimental determination of solar radiation at this location could have provided more validity for this analysis.

Vuwani Region of Limpopo Province in South Africa is a suitable place for outdoor tests with tropical climate and long sunshine hours. However, hot temperatures produce less efficient photo conversion for mono-crystalline solar cells. The peak power for mono-crystalline solar cell decreases as the operating temperature of cells increases. For the same irradiance level, the output power, and therefore the efficiency, decreases with the increasing cell temperature.
It can be concluded that the mono-crystalline PV array installed in the present study area may be used under outdoor conditions for small scale electricity needs in rural settings of Vhembe district.

4.3. REFFERENCES

[1] Zh. Peidon et al. / Renewable and Sustainable Energy Reviews 13 (2009) 439–449
[2] Eliot D: 1997.Energy society and environment Routledge.
[3] K. Sopian et al. / Renewable and Sustainable Energy Reviews 15 (2011) 4706– 4725.
[4] M. Zengetal. /Renewable and Sustainable Energy Reviews20 (2013)36–44
[5] Feyman, 1966: Lectures on Physics, mainly mechanics, radiation and heat, Feyman, Richard.
[6] International Energy Agency: 2007. Renewables in global energy supply: An IEA fact sheet,
[7] A. Tolón-Becerra et al. / Renewable Energy 36 (2011) 2067e2077
[8] Concise encyclopedia of material for energy systems, 2009. Elsevier Ltd, Oxford, UK.
[9] SA year book: 2007/08. Minerals, energy and geology.
[10] South African energy synopsis: 2010.Department of mineral and energy of South Africa.
[11] Http://www.energy.gov.za/files/electricity_frame.htmlaccessed in 2009
[12] Http://www.csir.co.za/enews/2007 set/dpss01.htmlaccessed in 2008

[13 Census 2011, Census in brief: 2012 / Statistics South Africa, Pretoria

[14] Donald Aitken: 2003 .White paper, transitioning to a renewable energy future

[15] Http://mynasa.nasa.gov/worldbook/sun worldbook.html, accessed online 1n 2008

[16] World meteorological organization: 1999.Measurement of solar radiation.

[17] AAM Sayigh: 1991. Generating electricity from the sun Pergamon PLC

[18] Jenny Nelson: 2009.The physics of solar cells, Imperial College press, London.

[19] Richard J. Komp: 2001. Practical photovoltaics: electricity from solar cells, third edition aatec publications.

[20] A.E. Schwaller and Gilbert A.F: 1980. Energy Technology Source of power: Thomson learning Tools an International Thomson Publishing Company, New York.

[21] Homer, energy LCC: 2009. The micro power optimization model, 885 Arapahoe ave.

[22] DS-TRACER user's manual: 2006

[23] Delta-t weather station user manual

[24] Flex max60 maximum power point tracking charge controller user's manual,2008.

[25] Http//www. Mrsolar.com//what-is-maximum-power-point-tracking.php.htm.accesed in 2011

[26] A. Angstrom: 1924, Solar and terrestrial radiation. Q.J.R. Meteorol. Soc, Vol. 50: 121-125.

[27] M. A Wohab: 1993, New approach to estimate Angstrom coefficients. Solar Energy, Vol. 51: 241-245.

[28] HP Garg and J Prakash: 2002, Solar Energy fundamentals and applications. Tata McGraw-Hill Publishing Company Limited, New Delhi.

[29] G D Rai:2009, Solar Energy Utilization. Khanna Publishers

[30] C Frohlich and RW Brusa:1981, Solar radiation and its variation in time. Sol Physics, Vol. 74: 209-215.

[31] AA El-Sebaii and AATrabea:2005, Estimation of global solar radiation on horizontal surfaces over Egypt. J. Solids, Vol. 28 (1).

[32] PI Cooper: 1969, The absorption of solar radiation in solar stills: Solar Energy, Vol. 12 (3): 333-346.